Title

Measurement of the underlying event in jet events from 7 TeV proton—proton collisions with the ATLAS detector

Journal

European Physical Journal C, 74(8)

ISSN

1434-6044

Authors

The ATLAS Collaboration

Aad, G

Abajyan, T

et al.

Publication Date

2014-08-01

DOI

10.1140/epjc/s10052-014-2965-5

Eur. Phys. J. C (2014) 74:2965
DOI 10.1140/epjc/s10052-014-2965-5

THE EUROPEAN PHYSICAL JOURNAL C

Regular Article - Experimental Physics

Measurement of the underlying event in jet events from 7 TeV proton–proton collisions with the ATLAS detector

The ATLAS Collaboration[⋆]

CERN, 1211 Geneva 23, Switzerland

Received: 3 June 2014 / Accepted: 2 July 2014 / Published online: 12 August 2014

Abstract Distributions sensitive to the underlying event in QCD jet events have been measured with the ATLAS detector at the LHC, based on 37 pb^{-1} of proton–proton collision data collected at a centre-of-mass energy of 7 TeV. Charged-particle mean p_{T} and densities of all-particle E_{T} and charged-particle multiplicity and p_{T} have been measured in regions azimuthally transverse to the hardest jet in each event. These are presented both as one-dimensional distributions and with their mean values as functions of the leading-jet transverse momentum from 20 to 800 GeV. The correlation of charged-particle mean p_{T} with charged-particle multiplicity is also studied, and the E_{T} densities include the forward rapidity region; these features provide extra data constraints for Monte Carlo modelling of colour reconnection and beam-remnant effects respectively. For the first time, underlying event observables have been computed separately for inclusive jet and exclusive dijet event selections, allowing more detailed study of the interplay of multiple partonic scattering and QCD radiation contributions to the underlying event. Comparisons to the predictions of different Monte Carlo models show a need for further model tuning, but the standard approach is found to generally reproduce the features of the underlying event in both types of event selection.

1 Introduction

To perform precise measurements or search for new physics phenomena at hadron colliders it is essential to have a good understanding not only of the hard scattering process, but also of the accompanying interactions of the rest of the proton. The aspects of a given collider event not identified with the hard process are collectively termed the "underlying event" (UE). The UE can receive contributions not only from additional partonic scatters in the same proton–proton collision (multiple parton interactions, or MPI) and from quantum chromodynamics (QCD) colour connections between partons and beam remnants, but also from processes typically associated with the hard process, such as QCD initial- and final-state radiation (ISR, FSR). It is impossible, even in principle, to unambiguously separate the UE from the hard scattering process on an event-by-event basis. However, observables can be measured which are particularly sensitive to its properties.

The low-momentum QCD processes which dominate the UE are the main type of interaction in proton–proton collisions. The behaviour of such soft interactions cannot be calculated reliably with perturbative QCD methods, due to the divergence of the QCD coupling at low scales; it is therefore typically modelled in a phenomenological manner by Monte Carlo (MC) event generator programs. These models invariably contain parameters whose values are not a priori known or calculable and must instead be fitted ("tuned") to experimental data. Predictivity of UE modelling is important since the UE forms an irreducible background of particle activity in all hard-scale processes studied at the LHC. Most new-physics searches operate in event types with high momentum transfer where the UE has not yet been measured, hence extension of the measurements into these regions is important, as is testing the reliability of the UE modelling between hard process types with different QCD colour flows.

UE observables were previously measured by both the Tevatron and LHC experiments. The CDF experiment measured the UE with inclusive jet and Drell–Yan events in Tevatron proton–antiproton ($p\bar{p}$) collision data, at centre-of-mass energies of $\sqrt{s} = 1.8$ TeV [1] and 1.96 TeV [2]. The ATLAS [3–6], ALICE [7] and CMS [8,9] experiments at the LHC have thus far measured observables sensitive to the UE in proton–proton (pp) collision data at $\sqrt{s} = 900$ GeV and 7 TeV, using track-jets, leptonically decaying Z bosons, and the highest-p_{T} charged particle to define the hard scattering direction in the event. This paper reports a measurement of UE observables in inclusive jet and exclusive dijet events, recorded by the ATLAS detector [10] at the LHC using proton–proton collisions at a centre-of-mass energy of 7 TeV, from the LHC 2010 run. This study extends the phase-

⋆ e-mail: atlas.publications@cern.ch

space coverage of previous studies of the UE by probing a much higher jet-p_{T} scale (up to 800 GeV), studying a subset of events with an exclusive dijet topology, and by measuring the sum of the transverse energy in the full range of the ATLAS calorimeter acceptance.

This paper is organised according to the following structure. The ATLAS detector is described in Sect. 2. The observables sensitive to the underlying event are defined in Sect. 3. In Sect. 4, the QCD MC models used in this analysis are discussed. Sections 5–7 respectively describe the event selection, correction of the data back to particle level, and estimation of the systematic uncertainties. The results are discussed in Sect. 8 and finally the conclusions are presented in Sect. 9.

2 The ATLAS detector

The ATLAS detector is described in detail in Ref. [10]. In this analysis, the trigger system, the tracking detectors, and the calorimeters are of particular relevance.

The ATLAS inner detector is immersed in the 2 T axial magnetic field of a superconducting solenoid, and measures the trajectories of charged particles in the pseudorapidity range $|\eta| < 2.5$ with full azimuthal coverage.[1] The inner detector consists of a silicon pixel detector (pixel), a silicon microstrip detector (SCT) and a straw-tube transition radiation tracker (TRT). The inner detector barrel (endcap) detectors consist of 3 (2×3) pixel layers, 4 (2×9) layers of double-sided silicon strip modules, and 73 (2×160) layers of TRT straws. The pixel, SCT and TRT have r–ϕ position resolutions of 10, 17, and 130 μm respectively, and the pixel and SCT have z-coordinate (r-coordinate) resolutions of 115 and 580 μm respectively in the barrel (endcaps). A track traversing the barrel typically has 11 silicon hits (3 pixel clusters, and 8 strip clusters), and more than 30 straw tube hits.

Electromagnetic (EM) calorimetry is provided by liquid-argon (LAr) calorimeters. The barrel ($|\eta| < 1.475$) and endcap ($1.375 < |\eta| < 3.2$) sections have lead absorbers, and the forward ($3.1 < |\eta| < 4.9$) section (FCal) contains LAr/Cu modules. The hadronic calorimeter is divided into four sections: the barrel ($|\eta| < 0.8$) and extended barrel ($0.8 < |\eta| < 1.7$), both of which are scintillator/steel sampling calorimeters; the hadronic endcap ($1.5 < |\eta| < 3.2$), which has LAr/Cu modules; and the hadronic FCal, which has LAr/W modules and covers the same η range as the EM FCal. The total calorimeter coverage is $|\eta| < 4.9$.

[1] ATLAS uses a right-handed coordinate system with its origin at the nominal interaction point (IP) in the centre of the detector and the z-axis along the beam pipe. The x-axis points from the IP to the centre of the LHC ring, and the y-axis points upward. Cylindrical coordinates (r, ϕ) are used in the transverse plane, ϕ being the azimuthal angle around the beam pipe. The pseudorapidity is defined in terms of the polar angle θ as $\eta = -\ln\tan(\theta/2)$.

The EM calorimeter has three longitudinal layers (called strip, middle and back) and a fine segmentation in the lateral direction of the showers within the inner detector coverage. At high energy, most of the EM shower energy is collected in the middle layer which has a η–ϕ granularity of $\eta \times \phi = 0.025 \times 0.025$. The η–ϕ granularity in the hadronic endcap ranges from $\eta \times \phi = 0.1 \times 0.1$ to 0.2×0.2. In the forward calorimeter, the cells are not arranged in projective towers but are instead aligned parallel to the beam axis. As such the readout granularity is not constant in η–ϕ.

The ATLAS detector has a three-level trigger system: level 1, level 2 and the event filter. Data were taken for this analysis using the single-arm minimum bias trigger scintillators (MBTS) and central jet-trigger, covering $|\eta| < 3.2$. The MBTS are mounted at each end of the detector in front of the liquid-argon endcap-calorimeter cryostats at $z = \pm 3.56$ m and are segmented into eight sectors in azimuth and two rings in pseudorapidity ($2.09 < |\eta| < 2.82$ and $2.82 < |\eta| < 3.84$). Events were triggered by the MBTS system if at least one hit from either side of the detector was recorded above threshold.

3 The underlying event observables

The UE observables presented in this paper are constructed separately from charged-particle tracks with $p_{\mathrm{T}} > 0.5$ GeV and from three-dimensional clusters of calorimeter cells [11].

Tracks are required to be within $|\eta| < 2.5$ for all observables by the acceptance of the ATLAS tracker, while clusters are constructed separately for pseudorapidity acceptances of $|\eta| < 4.8$ and $|\eta| < 2.5$ to provide one measurement with full forward coverage and one compatible with the more restricted acceptance of the tracker.

These detector-level objects were corrected to hadron-level quantities (i.e. in terms of particles with a mean proper lifetime $\tau > 0.3 \times 10^{-10}$ s either directly produced in the pp interactions or in the decay of particles with a shorter lifetime) using the definitions given in Refs. [3,6]. The jet correction to hadron level is based on charged and neutral particles with this lifetime cut, excluding neutrinos. The selected tracks were corrected to primary charged particles with $p_{\mathrm{T}} > 0.5$ GeV and $|\eta| < 2.5$. No attempt was made to identify single calorimeter cell clusters (according to the ATLAS definition [11]) with primary particles, but momentum sums of clusters were corrected to momentum sums of primary charged particles with momentum $p > 0.5$ GeV and primary neutral particles (including neutrinos) with $p > 0.2$ GeV. A geometric requirement of $|\eta| < 4.8$ or $|\eta| < 2.5$ was applied depending on the cluster observable. Lower-momentum particles were not included because detector simulation indicated that they do not deposit significant energy in the ATLAS calorimeters, due to interactions with detector material at

Table 1 Definition of the observables measured in each event at hadron and detector level. The hadron-level observables based on momentum use only particles with $p_{\mathrm{T}} > 0.5$ GeV, and those based on energy use $p > 0.5$ GeV for charged particles and $p > 0.2$ GeV for neutral particles. All hadron-level definitions are based on particles with mean proper lifetime $\tau > 0.3 \times 10^{-10}$ s. Tracks are selected if they satisfy the criteria described in Sect. 5. In the profile plots shown later, these per-event observables are averaged over the events in each bin of the profile (i.e. in $p_{\mathrm{T}}^{\mathrm{lead}}$ or N_{ch}). The event-ensemble averages shown in the profiles are indicated with $\langle\cdot\rangle$ notation, hence the form "mean p_{T}" is used to distinguish the per-event mean p_{T} which is profiled as the double mean, $\langle$mean $p_{\mathrm{T}}\rangle$. The trans-max and trans-min sub-regions are defined per-event and are also specific to the observable being considered

Event-wise observable	Particle level	Detector level
$p_{\mathrm{T}}^{\mathrm{lead}}$	Transverse momentum of the leading jet	
$N_{\mathrm{ch}}/\delta\eta\,\delta\phi$	Number of stable charged particles per unit $\eta-\phi$	Number of selected tracks per unit $\eta-\phi$
$\sum p_{\mathrm{T}}/\delta\eta\,\delta\phi$	Scalar p_{T} sum of stable charged particles per unit $\eta-\phi$	Scalar p_{T} sum of selected tracks per unit $\eta-\phi$
Mean p_{T}	Mean p_{T} of stable charged particles (at least one charged particle is required)	Mean p_{T} of selected tracks (at least one selected track is required)
$\sum E_{\mathrm{T}}/\delta\eta\,\delta\phi$	Scalar E_{T} sum of stable charged and neutral particles per unit $\eta-\phi$	Scalar E_{T} sum of selected calorimeter energy clusters per unit $\eta-\phi$

smaller radii and bending in the magnetic field. Since the properties of low-momentum particles are not well known or modelled, excluding them from the hadron-level phase space definition reduces the model dependence of the correction procedure.

The observables used in this study, defined in Table 1, employ the conventional UE azimuthal division of events into regions relative to the direction of the "leading" object in the event [1]. The leading object in this case is defined by the anti-k_t [12] jet with distance parameter $R = 0.4$ which has the largest p_{T} (denoted by $p_{\mathrm{T}}^{\mathrm{lead}}$) after application of the jet selection criteria described in Sect. 5. At hadron level the jets are constructed from primary particles as previously defined, excluding neutrinos. The azimuthal regions are defined with respect to the ϕ of the leading jet: a 120° "towards" region surrounds the leading jet, an "away" region of the same size is azimuthally opposed to it and two "transverse" regions each of 60° are defined orthogonal to the leading jet direction. This is illustrated in Fig. 1, which displays the azimuthal distance from the leading jet, $|\Delta\phi|$, used to define the UE regions.

Since the towards region is dominated by the leading jet and the away region by the balancing jet (in the dominant dijet configuration), the transverse regions are the most sensitive to accompanying particle flow, i.e. the UE. In addition, the transverse regions may be distinguished event-by-event based on which one has more or less activity, named the "trans-max" and "trans-min" sides respectively. The trans-max side is more likely to be affected by wide-angle emissions associated with the hard process and correspondingly the trans-min observables have the potential to be more sensitive to soft MPI and beam-remnant activity. In this analysis, the trans-min/max definition is specific to the observable being considered; for example the trans-max side for the charged-particle multiplicity (N_{ch}) observable (i.e. the side of the transverse region which contains more charged particles)

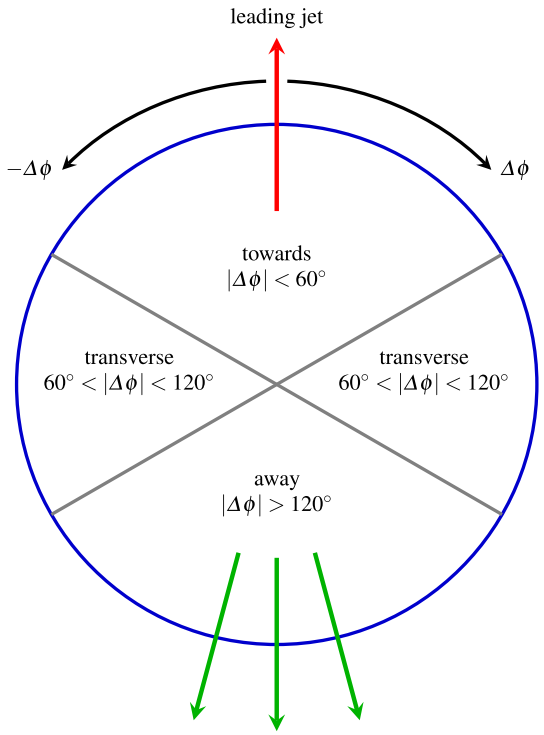

Fig. 1 Definition of regions in the azimuthal angle with respect to the leading jet. The towards, away and transverse regions are defined in the text. The balancing parts of the jet system are indicated with *green arrows*, compatible with the dominant dijet event topology. Multi-jet topologies, encountered in the inclusive jet event selection, are expected to contribute more substantially to the transverse regions than the geometry shown here

can be different from the trans-max side for the scalar sum of the particle transverse momentum ($\sum p_{\mathrm{T}}$) observable in the same event. The difference between trans-max and trans-min sides for a given observable is referred to as the "trans-diff" of that observable [13,14]. The trans-diff observables are very sensitive to hard initial- and final-state radiation.

This azimuthal segmentation of events around the leading-jet direction is based on an assumption of dominant dijet topologies. Measurements of LHC jet rates [15] indicate that events with three or more jets contribute to inclusive jet UE observables; hence there are substantial contributions to the transverse regions from the hard partonic scattering. While this subverts the intent of the azimuthally segmented observable definitions, the resulting interplay of hard and soft event features is itself interesting and relevant to modelling of hard pp interaction processes at the LHC. Hence, the transverse-region UE observables are studied both in inclusive jet events where multi-jet topologies contribute, and in the subset of exclusive dijet events where higher-order emissions beyond the leading dijet configuration are explicitly suppressed.

The particle and energy flow observables in the transverse regions are studied both as one-dimensional distributions, relatively inclusive in the properties of the hard process, and as "profile" histograms which present the dependence of the mean value of each observable (and its uncertainty) as a binned function of a hard process property, usually $p_{\mathrm{T}}^{\mathrm{lead}}$.

4 Monte Carlo models of the underlying event

In scattering processes modelled by perturbative QCD two-to-two partonic scatters, at sufficiently low p_{T} the partonic jet cross-section exceeds that of the total hadronic cross-section. This apparent problem is resolved by extending the single-hard-scatter model to include the possibility of multiple partonic scatters in a given hadron–hadron interaction. In this picture, the ratio of the partonic jet cross-section to the total cross-section is interpreted as the mean number of parton interactions in such events. This model is implemented in several Monte Carlo event generators, augmented in each implementation by various phenomenological extensions [16–20].

This analysis uses simulated inclusive jet events created by the Pythia 6 [16], Pythia 8 [17], Herwig+Jimmy [21], Herwig++ [18,22], Alpgen+Herwig+Jimmy [23], and Powheg+Pythia 6 [24] event generators. All but the last of these are leading-order parton shower generators, but use different hadronisation models and different parton shower formalisms; the Pythia family uses a hadronisation model based on the Lund string and a p_{T}- or virtuality-ordered parton shower, while Herwig+Jimmyand Herwig++ implement a cluster hadronisation scheme and their parton showers are ordered in emission angle.[2] The Fortran Herwig [21] generator by itself does not simulate multiple partonic interactions; these are added by the Jimmy [25] package. The Alpgen generator provides leading-order multi-leg matrix element events, i.e. it includes more complex hard process topologies than those used by the other generators but omits loop-diagram contributions. The Alpgen partonic events are showered and hadronised by the Herwig+Jimmy generator combination, making use of MLM matching [23] between the matrix element and parton shower to avoid double-counting of jet production mechanisms. A related matching process is used to interface Pythia 6 to the next-to-leading-order (NLO) Powheg generator, where the matching scheme avoids both double-counting and NLO subtraction singularities. The Powheg matrix element simulates the partonic dijet process at NLO, i.e. including the loop correction, while the third (real emission) partonic jet is calculated at leading order. Revision r2169 of Powheg is used; this version contains an important modification to the original Powheg dijet matching which reduces the incidence of spikes in physical distributions [26,27].

Such models typically introduce several parameters, which are to be tuned to data at different centre-of-mass energies and for a variety of hadronic processes. MC tuning in recent years has made extensive use of ATLAS and Tevatron underlying event and minimum bias data for a variety of event generators, most notably the Pythia and Herwig families. In this study we have used tuned MC generators both for data correction and systematic uncertainties, and for comparison to the detector-corrected data observables. The combinations of generators, PDFs and tunes are listed in Table 2. No currently available tunes make use of UE data from a pp initial state and high-p_{T} jet events as measured here, so the comparisons of corrected data to MC models give a good indication of the level of predictivity of models tuned to Tevatron or low-p_{T} LHC data.

The AMBT1 tune (ATLAS Minimum Bias Tune 1) [37] of Pythia 6 was the first LHC-data tune constructed by ATLAS, and primarily used diffraction-suppressed observables from the early ATLAS minimum bias (MB) measurements [40] as input to the tuning.

Perugia 2011 [30] is the latest in the "Perugia" set of Pythia 6 tunes, which use early LHC minimum bias and underlying event data and the Pythia p_{T}-ordered parton shower. A consistent definition of the strong coupling α_{S} is used throughout the parton showers for smooth interfacing to multi-leg matrix element generators, particularly Alpgen. This tune uses the CTEQ5L1 PDF [31].

The Pythia 6 DW [32] tune uses a virtuality-ordered parton shower and an MPI model not interleaved with the ISR. This tune was constructed to describe CDF Run II underlying event and Drell–Yan data and also uses the leading-order CTEQ5L1 PDF; it is included here for comparison to previous results.

Pythia 6 is also used in conjunction with a matched Powheg NLO matrix element using the CT10 PDF set, as

[2] The Pythia showers include an angular veto on the first ISR emission to approximate the colour coherence effect implicit in the Herwig angular ordering. The Herwig++ shower additionally uses massive splitting functions for heavy-quark emissions.

Table 2 Details of the MC models used in this paper. It should be noted that all tunes use data from different experiments for constraining different processes, but for brevity only the data which had most weight in each tune is listed. A "main data" value of "LHC" indicates data taken at $\sqrt{s} = 7$ TeV, although $\sqrt{s} = 900$ GeV data were also included with much smaller weight in the ATLAS tunes. Some tunes are focused on describing the minimum bias (MB) distributions better, while the rest are tuned to describe the underlying event (UE) distributions, as indicated in "focus". The detector-simulated MC configurations used for data correction are separated from those used in the results comparison plots, for clarity. For the POWHEG+PYTHIA 6 entry, separate parton distribution functions (PDFs) were used for the matrix element and parton shower/multiple scattering aspects of the modelling, indicated with "ME" and "PS/MPI" respectively

Generator	Version	Tune	PDF	Focus	Main data	Used for
PYTHIA 8	8.157	AU2 [28]	CT10 [29]	UE	LHC	MC/data comparison
PYTHIA 6	6.425	Perugia 2011 [30]	CTEQ5L [31]	UE	LHC	MC/data comparison
PYTHIA 6	6.421	DW [32]	CTEQ5L	UE	Tevatron	MC/data comparison
HERWIG++	2.5.1	UE7-2 [33]	MRST LO** [34]	UE	LHC	MC/data comparison
HERWIG+JIMMY	6.510	AUET2 [35]	MRST LO**	UE	LHC	MC/data comparison
ALPGEN+HERWIG+JIMMY	2.13 + 6.510	AUET1 [35]	CTEQ6L1 [36]	UE	LHC	MC/data comparison
POWHEG+PYTHIA 6	r2169 + 6.425	Perugia 2011	CT10 (ME) + CTEQ5L (PS/MPI)	UE	LHC	MC/data comparison
PYTHIA 6	6.425	AMBT1 [37]	MRST LO* [38]	MB	Early LHC	Data correction
HERWIG++	2.5.0	LO*_JETS [39]	MRST LO*	UE	Tevatron	Correction systematics

this is the highest perturbative order of QCD jet event modelling currently available in fully showered/hadronised form. The Perugia 2011 tune of PYTHIA 6 is used to shower these POWHEG events. While commonly used together, the Perugia 2011 tune was constructed based on leading-order matrix elements only, and without the POWHEG matching modification to the parton shower; the interest in comparing this model to data is hence to observe whether the POWHEG+PYTHIA 6 matching procedure has any adverse effect on UE distributions relative to standalone PYTHIA 6.

PYTHIA 8 adds to the established PYTHIA-family MPI model by interleaving not only the ISR emission sequence with the MPI scatterings, but also the FSR; all three processes compete against each other for emission phase space in the resulting evolution. The AU2 CT10 tune [28] used here is the variant of the latest ATLAS PYTHIA 8 UE tune set intended for use with the NLO CT10 PDF [29]. This configuration is the standard setup for jet event simulation in current ATLAS production use, with the model tuned to give a very good description of leading-track UE data at $\sqrt{s} = 7$ TeV.

Two tunes of HERWIG+JIMMY are used in this study: the ATLAS AUET2 LO** tune for standalone HERWIG+JIMMY, and the older AUET1 CTEQ6L1 used in the ALPGEN sample [35]. For HERWIG++ the standard 7 TeV underlying event tune UE7-2 [33] for the MRST LO** PDF is used. This model includes a colour reconnection model—the first for a cluster hadronisation generator—and provides a good description of both leading-track UE and minimum bias data at 7 TeV. The LO** PDF, like the LO* PDF used in the PYTHIA 6 AMBT1 sample, is one of a series of "modified leading order" PDFs which attempt to mimic full NLO simulated event characteristics by relaxation of PDF momentum sum rules and use of a p_{T}^2-based factorisation scale for better compatibility with the approximate resummation inherent in parton shower algorithms.

The PYTHIA 6 AMBT1 and HERWIG++ 2.5.0 samples were processed through the ATLAS detector simulation framework [41], which is based on GEANT4 [42], then reconstructed and analysed similarly to the data. These reconstructed events were used to calculate detector acceptances and efficiencies, to correct the data for detector effects. The fully simulated and reconstructed samples include overlay of MC pile-up events, simulated using PYTHIA 8 with the AM2 tune [43], with the mean number of interactions distributed according to data conditions. The HERWIG++ sample used for unfolding (i.e. correction of residual detector effects) was generated using HERWIG++2.5.0 with the default LO*_JETS [39] tune—an older configuration than that shown in the physics comparison plots in this paper. All other MC models described are used at the generated stable particle level only.

5 Data analysis object selection

This analysis uses the full ATLAS 2010 dataset of jet events in proton–proton collisions at $\sqrt{s} = 7$ TeV, in which the average number of multiple pp interactions per bunch crossing ("pile-up") was much smaller than in the 2011 data-taking period. Basic requirements on data quality and the operating conditions of the beam, the relevant sub-detectors and the triggers resulted in a dataset corresponding to an integrated luminosity of $37 \pm 1.3\,\mathrm{pb}^{-1}$, uncorrected for trigger prescales [44].

To select jet events, two different trigger systems were used: the MBTS trigger and the central jet-triggers, the latter of which has several p_{T} thresholds. The MBTS trigger selects

events containing charged particles within the fiducial acceptance of the minimum bias trigger scintillator, and was used to select events with jets having transverse momenta in the range 20–60 GeV. Jets with p_{T} greater than 60 GeV are above the threshold of full efficiency of the calorimeter-based jet-trigger, hence this was used to select jet events above this scale. A single jet-trigger was used for each $p_{\mathrm{T}}^{\mathrm{lead}}$ bin in the observables, specifically the fully efficient (>99 %) trigger with the smallest possible prescale factor for that bin [45].

To reject events due to cosmic-ray muons and other non-collision backgrounds, events were required to have at least one reconstructed "primary" pp interaction vertex, each having at least five tracks satisfying the following criteria [40]:

- $p_{\mathrm{T}} > 0.5$ GeV;
- $|\eta| < 2.5$;
- a minimum of one pixel and six SCT hits;
- a hit in the innermost pixel layer, if the corresponding pixel module was active;
- transverse and longitudinal impact parameters with respect to primary vertex $|d_0| < 1.5$ mm and $|z_0| \sin\theta < 1.5$ mm;
- for tracks with $p_{\mathrm{T}} > 10$ GeV, a χ^2 probability of track fit greater than 0.01 was required in order to remove mis-measured tracks.

Events with $p_{\mathrm{T}}^{\mathrm{lead}} < 100$ GeV were taken in conditions with negligible pile-up, while the bulk of events with higher $p_{\mathrm{T}}^{\mathrm{lead}}$ were taken in the second 2010 data-taking period, with a mean of 2–3 pp interactions per bunch crossing. To reduce the contributions from pile-up, events containing more than one reconstructed primary vertex with at least two associated tracks were removed.

Finally, to obtain an inclusive jet event selection, each event was required to contain at least one jet with $p_{\mathrm{T}} > 20$ GeV and rapidity $|y| < 2.8$. The resulting sample was entirely dominated by pure QCD jet events. For the exclusive dijet event selection an additional requirement of one and only one subleading jet was made, where the subleading jet had to pass the same cuts as the leading jet and also have $p_{\mathrm{T}} > 0.5\, p_{\mathrm{T}}^{\mathrm{lead}}$ and $|\Delta\phi| > 2.5$ to the leading jet. The same exclusive dijet cut was applied to the particle level MC samples, where appropriate, in addition to the requirements given in Sect. 3.

In both selections the jets were corrected to account for the calorimeters' response to the deposited energy.

Around 429,000 and 99,000 events were selected for the inclusive jet and exclusive dijet selections respectively.

6 Correction to particle level

To allow comparison of these results with theoretical predictions and other experimental studies, the underlying event distributions need to be corrected for selection efficiencies and detector resolution effects. A two-step correction procedure was used, where first the track efficiency corrections were applied for the track-based observables, then the remaining detector effects were unfolded to produce observables at particle level which may be directly compared to MC model predictions.

6.1 Track reconstruction efficiency and cluster calibration

The efficiency of the ATLAS detector to reconstruct a charged particle as a track was measured in a previous analysis [40], with the same track selection as used here. Each track was reweighted by the inverse of this efficiency, which also accounts for the contributions of tracks reconstructed from secondary particles, and particles whose true kinematics were outside the kinematic range (OKR) of the selection but which were reconstructed within the acceptance cuts due to detector resolution. For tracks with $p_{\mathrm{T}} > 500$ MeV, the effects of fake tracks (those constructed from tracker noise and/or hits which were not produced by a single particle) and OKR migrations were found to be negligible.

For cluster-based observables, both the hadronic and electromagnetic calorimeter cell clusters were used, with calibrations as described in Refs. [46] and [11]. The cluster energy was corrected to the momentum of the charged or neutral hadron, and the simulation was validated using the diphoton invariant mass distribution, $M_{\gamma\gamma}$, for $\pi^0 \to \gamma\gamma$ candidates [6].

6.2 Unfolding

Bayesian iterative unfolding [47] was used to correct for residual detector resolution effects, using the Imagiro 0.9 software package [48].

The Bayesian iterative unfolding method requires two inputs: a prior probability distribution for the observable (the MC generator-level distribution is used for this), and a smearing matrix which relates the measured distribution of an observable to its hadron-level distribution. The smearing matrix element S_{ij} is the probability of a particular event from bin i of the hadron-level distribution being found in bin j of the corresponding reconstructed distribution, as calculated using MC samples. For the profile histogram observables in this paper, a two-dimensional (2D) histogram was created with dense binning in the observable whose evolution is being profiled, such that each unfolding bin corresponds to a 2D range in e.g. $p_{\mathrm{T}}^{\mathrm{lead}}$ vs. $\sum p_{\mathrm{T}}$ space: the 2D nature of the bin has no effect on the mathematics of the unfolding procedure. Migrations involving the $p_{\mathrm{T}}^{\mathrm{lead}} < 20$ GeV region, excluded from the analysis phase space, were handled in detail for the unfolding of observables binned in $p_{\mathrm{T}}^{\mathrm{lead}}$, but for other observables such in/out migrations were treated as

fake or missing events respectively; this was required because a more detailed approach would add an extra dimension to the smearing matrix, which would then be too statistically limited to be usable.

The unfolding process was iterated to avoid dependence on the prior probability distribution; the corrected data distribution produced in each iteration is used as the prior for the next. In this analysis, two iterations were performed since this gave the smallest residual bias when tested on MC samples while keeping the statistical uncertainties small. The central values of the data distributions corrected to hadron level were calculated using prior distributions and smearing matrices from the PYTHIA 6 AMBT1 MC sample.

7 Systematic uncertainties

Systematic uncertainties on the measured distributions were assessed using the same unfolding procedure as for the central values of the observables, but with the input $p_{\mathrm{T}}^{\mathrm{lead}}$, track and cluster p_{T} and track and cluster weights shifted by $\pm 1\sigma$ variations in each source of uncertainty.

The following sources of uncertainty are included:

Jet reconstruction: These uncertainties—dependent on the jet energy scale calibration procedure, the impact of pile-up on the jet energy, the jet reconstruction efficiency and the jet energy resolution—have been calculated as in Ref. [49]. For the UE observables profiled against leading-jet p_{T}, they add up to approximately 1 %.

Track reconstruction-efficiency uncertainty: Tracking efficiency uncertainties were studied in Ref. [40], the two largest being found to be due to the amount of material in the inner detector and the consequence of the χ^2 probability cut to remove misreconstructed tracks. The effect of uncertainties in the amount of material in the inner detector is a 2 % relative uncertainty in the efficiency in the barrel region, rising to over 7 % for $2.3 < |\eta| < 2.5$, for tracks with $p_{\mathrm{T}} > 500$ MeV. The maximum difference between the fraction of events in data and MC simulation which passed the χ^2 probability cut was found to be 10 %. This value was taken as a conservative estimate of the systematic uncertainty, and was applied to tracks with $p_{\mathrm{T}} > 10$ GeV only.

Cluster reconstruction efficiency: The accuracy with which the MC samples simulate the energy response of the calorimeters to low-energy particles was determined separately for electromagnetic and hadronic particles. An average is then obtained, using the PYTHIA 6 AMBT1 prediction of the relative contribution to $\sum E_{\mathrm{T}}$ by different particle types [6]. For electromagnetic particles the systematic uncertainty arises from the extraction of the energy scale from fits to the $M_{\gamma\gamma}$ distributions in $\pi^0 \to \gamma\gamma$ candidates. The total uncertainty depends on the $|\eta|$ region and is typically 2–4 %, but is as large as 15 % in the regions where different calorimeter subsystems overlap. The uncertainty in the energy response for hadronic particles in the central region ($|\eta| < 2.4$), where there is good coverage from the inner tracking detector, was obtained from studies of the ratio of the energy measured by the calorimeter to the track momentum measured by the inner detector for isolated charged particles and is within a few percent [49].

Pile-up and merged vertices: The effect of pile-up on the underlying event observables after the tight vertex selection was assessed using an MC sample with realistic modelling of the pile-up conditions in 2010 data; the largest deviation from the sample without pile-up was observed to be 1 %. A ± 1 % shift was hence applied to the values of all observable bins used as input to the unfolding, and the resultant shifts on unfolded observables have been used as the systematic uncertainty due to merged vertices. This uncertainty is less than 2 % for most bins, but increases to approximately 5 % at high $p_{\mathrm{T}}^{\mathrm{lead}}$.

Unfolding: The uncertainty due to model-dependence of the unfolding procedure was taken as the difference between the results of unfolding with each of the two MC samples, PYTHIA 6 AMBT1 and HERWIG++. The dominant effect arises from modelling of low p_{T} QCD radiation, which produces a typical uncertainty of 1 % but can reach 20 % at the edges of the fiducial phase space studied here. An additional uncertainty was estimated using two different priors: the unmodified generator-level distribution, and the generator-level distribution after reweighting so that the reconstructed distribution matches the data. This uncertainty is less than 1% throughout the fiducial phase space of the measurement.

Systematic uncertainty contributions from electronic noise and beam-induced background, simulation of the primary vertex position, and simulation of the trigger selection were also considered and were found to be negligible. Table 3 summarises the sizes of contributions to systematic uncertainties for the UE profile observables with both the inclusive jet and exclusive dijet selections. The $\langle$mean $p_{\mathrm{T}}\rangle$ vs. N_{ch} profile observables have flat symmetric uncertainties of 1 % each for unfolding and reconstruction efficiency, increasing to $\sim$10 % in the first and last bins of N_{ch}.

8 Results

This section presents and discusses the key distributions from this analysis, primarily profile observables of mean UE characteristics as functions of $p_{\mathrm{T}}^{\mathrm{lead}}$ (i.e. hard process scale), but

Table 3 Summary of systematic uncertainties for inclusive jet and exclusive dijet profiles vs. $p_{\mathrm{T}}^{\mathrm{lead}}$. The "efficiency" uncertainties include material uncertainties in the tracker and calorimeter geometry modelling. The "JES" uncertainty source for jets refers to the jet energy scale calibration procedure [49]

Quantity	Inclusive jets			Exclusive dijets		
	Pile-up and merged vertices			Pile-up and merged vertices		
All observables	1–3 %			1–5 %		
Charged tracks	Unfolding	Efficiency		Unfolding	Efficiency	
$\sum p_{\mathrm{T}}$	3 %	1–7 %		3–13 %	2–7 %	
N_{ch}	1–2 %	3–4 %		3–22 %	3–7 %	
mean p_{T}	1 %	0–4 %		1–9 %	1 %	
Calo clusters	Unfolding	Efficiency		Unfolding	Efficiency	
$\sum E_{\mathrm{T}}$, $\lvert\eta\rvert < 4.8$	2–3 %	4–6 %		5–21 %	4–9 %	
$\sum E_{\mathrm{T}}$, $\lvert\eta\rvert < 2.5$	3–5 %	4–6 %		1–21 %	4–7 %	
Jets	Energy resolution	JES	Efficiency	Energy resolution	JES	Efficiency
$p_{\mathrm{T}}^{\mathrm{lead}}$	0.3–1 %	1–4 %	0.1–2 %	0.4–3 %	1–3 %	0.3–3 %

also distributions of charged-particle $\sum p_{\mathrm{T}}$ and multiplicity density within bins of $p_{\mathrm{T}}^{\mathrm{lead}}$, and the correlation of transverse-region mean p_{T} with the charged-particle multiplicity.

In these plots, all observables are studied for both the inclusive jet and exclusive dijet event selections. The data, corrected to particle level, are compared to predictions of PYTHIA 6 with the Perugia 2011 and DW tunes, HERWIG+JIMMY with the AUET2 tune, PYTHIA 8 with the AU2 CT10 tune, HERWIG++ with the UE7-2 tune, ALPGEN+HERWIG+JIMMY with the AUET1 tune, and POWHEG+PYTHIA 6 with the Perugia 2011 tune.

To allow direct comparison between full transverse and trans-min/max/diff region quantities, between central and full-η cluster quantities, and to other experiments with different angular acceptances, the observables are presented as densities in $\eta-\phi$ space. Specifically, the raw quantities are divided by the total angular area of the region in which they were measured to produce the number, transverse momentum, and transverse energy densities: $N_{\mathrm{ch}}/\delta\eta\,\delta\phi$, $\sum p_{\mathrm{T}}/\delta\eta\,\delta\phi$, and $\sum E_{\mathrm{T}}/\delta\eta\,\delta\phi$ respectively. The central transverse-region observables are scaled by $\delta\eta\,\delta\phi = (2\times 2.5)\times(2\times\pi/3) = 10\pi/3$. The total transverse energy of charged and neutral particles, $\sum E_{\mathrm{T}}$, is defined using the full pseudorapidity range in the transverse region, so its area normalisation is $\delta\eta\,\delta\phi = (2\times 4.8)\times(2\times\pi/3) = 19.2\pi/3$. The trans-max, trans-min and trans-diff regions have only half of the corresponding transverse-region area since by definition they only consider one side in $\Delta\phi$.

8.1 Distributions of N_{ch} and $\sum p_{\mathrm{T}}$ densities

In Fig. 2 the distributions of N_{ch} and $\sum p_{\mathrm{T}}$ densities in the transverse, trans-max and trans-min regions, for the inclusive jet selection, are shown for $p_{\mathrm{T}}^{\mathrm{lead}}$ bins of 20–60 GeV, 60–210 GeV, and >210 GeV. This presentation displays the evolution of each distribution in bins of increasing $p_{\mathrm{T}}^{\mathrm{lead}}$, where each $p_{\mathrm{T}}^{\mathrm{lead}}$ bin is independently normalised to unity. For both the $\sum p_{\mathrm{T}}$ and N_{ch} density observables, particularly in the transverse and trans-max regions shown in the top two rows, the development of hard tails in the distributions is clearly seen as the $p_{\mathrm{T}}^{\mathrm{lead}}$ cut is increased. The trans-min region in the bottom row also shows evolution in the tails, but the total contribution to the normalisation from the tails is much less, as may be seen from the lack of $p_{\mathrm{T}}^{\mathrm{lead}}$ dependence in the peak height for the trans-min region plots as compared to the transverse and trans-max ones. The peak regions for both variables are narrower and biased toward low values for trans-min, and wider for trans-max.

These characteristics of $p_{\mathrm{T}}^{\mathrm{lead}}$ and region dependence, and the importance of tails at high values, indicate that extra jet activity is responsible for the changes in the transverse and trans-max region distributions, while the relative stability of the trans-min peak region against jet activity reflects the particular suitability of the trans-min region observables for measurement of the multi-parton scattering contribution to the UE.

8.2 Charged-particle $\sum p_{\mathrm{T}}$ and multiplicity densities vs. $p_{\mathrm{T}}^{\mathrm{lead}}$

In Fig. 3 the transverse region charged-particle multiplicity and $\sum p_{\mathrm{T}}$ density profiles are shown as functions of $p_{\mathrm{T}}^{\mathrm{lead}}$. For the inclusive jet events in the left column, the total transverse region activity increases with $p_{\mathrm{T}}^{\mathrm{lead}}$ according to both the mean $\sum p_{\mathrm{T}}$ and N_{ch} density measures. The exclusive dijet topology shown in the right column, where multi-jet

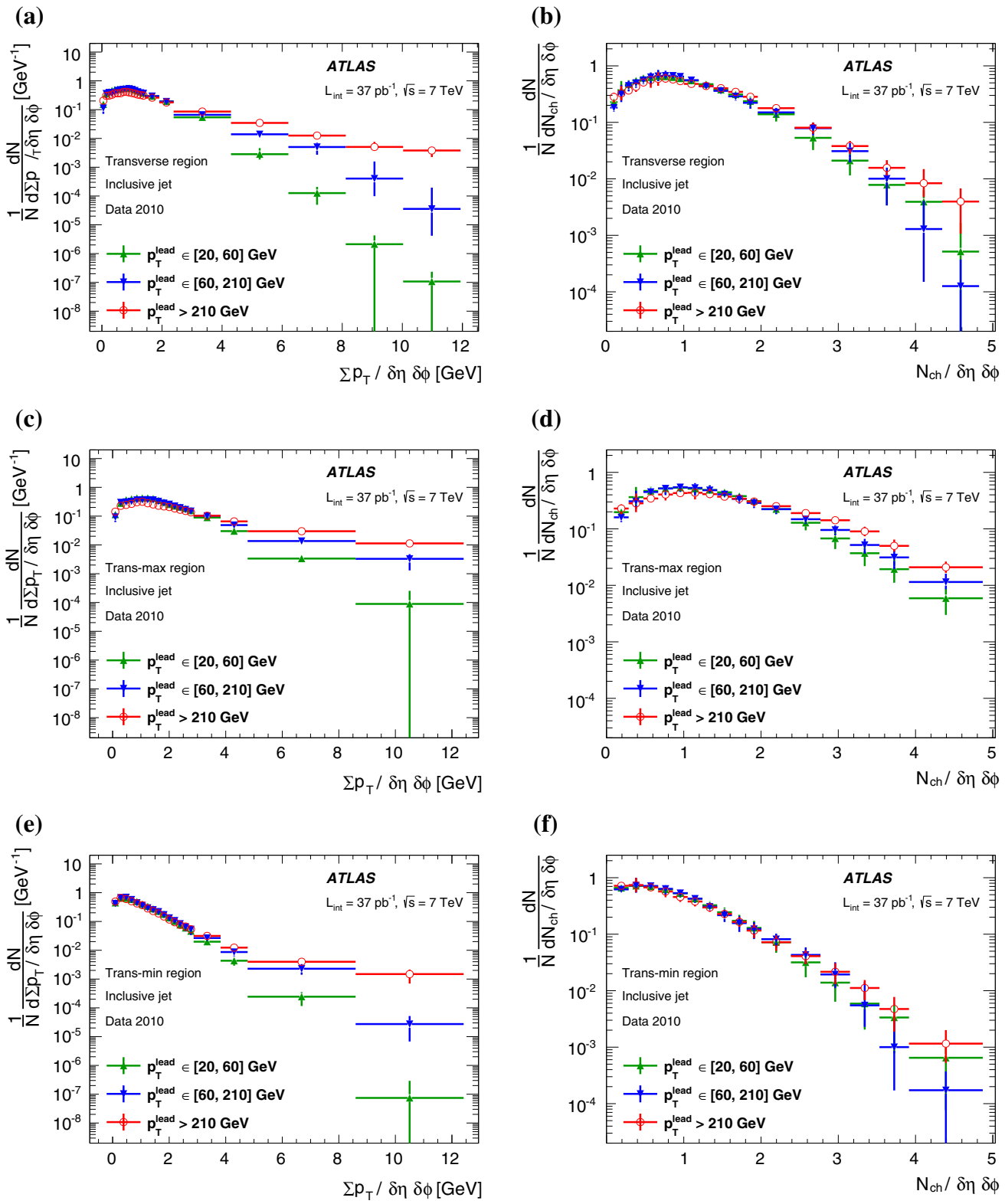

Fig. 2 Comparison of $\sum p_T$ (*left column*) and N_{ch} (*right column*) density distributions for different p_T^{lead} requirements, data only. The jets are required to have p_T of at least 20 GeV, and be within $|y| < 2.8$, whereas the charged particles have at least a p_T of 0.5 GeV and $|\eta| < 2.5$. The *top*, *middle* and *bottom rows*, respectively, show the transverse, trans-max and trans-min regions. Each p_T^{lead} slice is independently normalised to unity via division by the number of events in the slice, N. The *error bars* show the combined statistical and systematic uncertainty

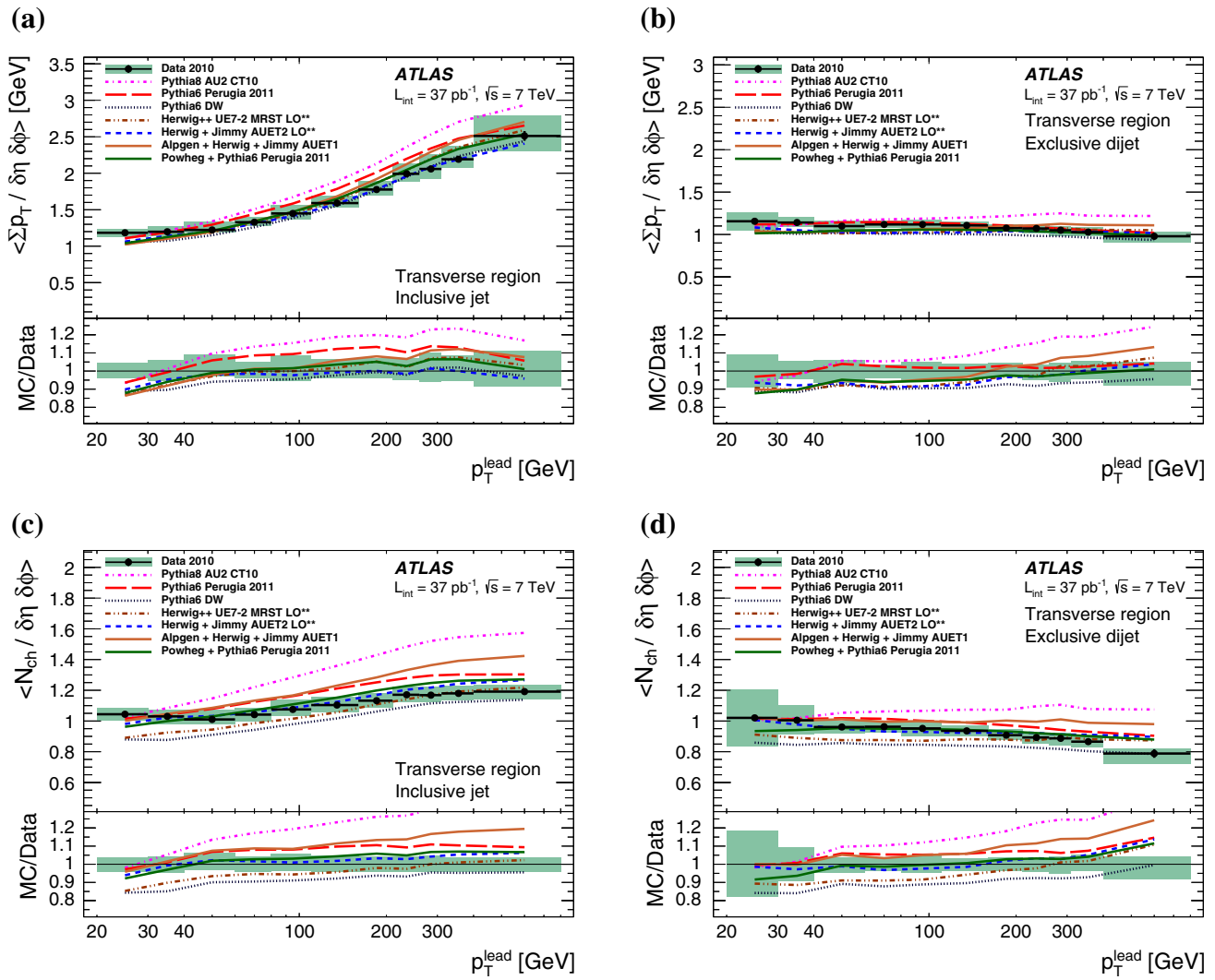

Fig. 3 Profiles of charged-particle $\sum p_{\mathrm{T}}$ (*top row*) and charged multiplicity (*bottom row*) densities against the leading-jet p_{T}, for the inclusive jet (*left column*) and exclusive dijet (*right column*) event selection. The jets are required to have p_{T} of at least 20 GeV, and be within $|y| < 2.8$, whereas the charged particles have at least a p_{T} of 0.5 GeV and $|\eta| < 2.5$. The total transverse-region activity is compared with several MC models, with the data *error bars* indicating the statistical uncertainty and the shaded area showing the combined statistical and systematic uncertainty

events are explicitly excluded, provides an alternative view of the same observables. The exclusive dijet $p_{\mathrm{T}}^{\mathrm{lead}}$ profiles are seen to decrease as $p_{\mathrm{T}}^{\mathrm{lead}}$ increases, although the dependence is much weaker than the opposite behaviour seen in the inclusive jet events. This behaviour is somewhat surprising and is not understood in detail, however we note that in addition to excluding events with extra jets from the hard process, the exclusive dijet requirement also excludes events with extra jets produced by MPI. This unavoidable consequence of the dijet cut may be responsible for the downward trend which is also seen in some MC predictions, particularly those from PYTHIA 6. The data are hence broadly consistent with modelling of the UE as independent of the hard process scale at the leading-jet p_{T} scales considered here. However the details of the data behaviour, in particular the decreasing transverse region activities with $p_{\mathrm{T}}^{\mathrm{lead}}$ in the exclusive dijet event selection are not fully understood.

The division of the transverse regions into per-event trans-max and trans-min sides, and the corresponding per-event differences between them, the "trans-diff" observables, are shown in Fig. 4. In the inclusive jet events, the trans-max activity (for both $\sum p_{\mathrm{T}}$ and N_{ch}) grows with $p_{\mathrm{T}}^{\mathrm{lead}}$, similarly to the full transverse-region trend, but its trans-min complement is almost constant over the whole range of $p_{\mathrm{T}}^{\mathrm{lead}}$. This observation is compatible with the interpretation of the trans-min region as being less affected by the hard part of the underlying event.

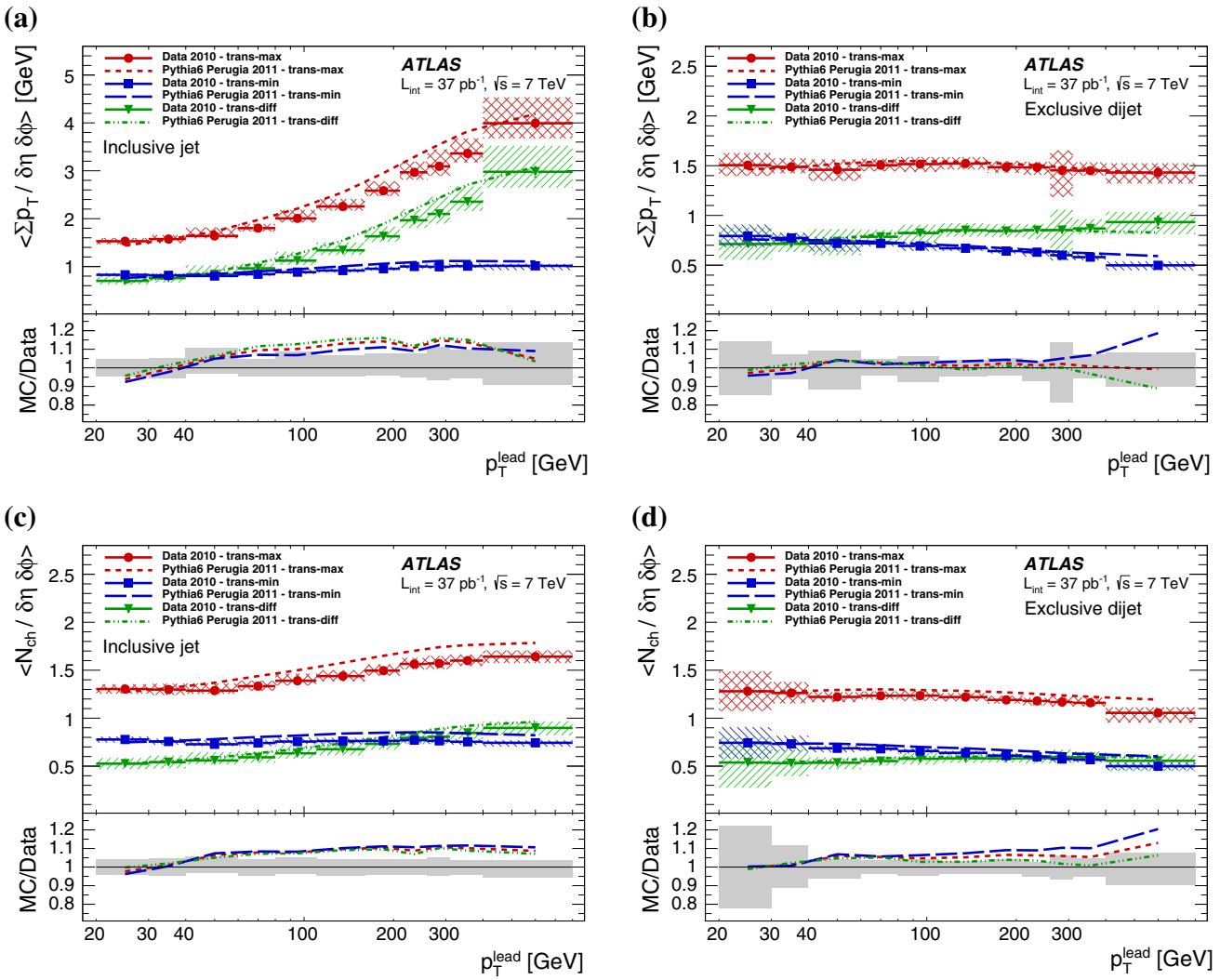

Fig. 4 Profiles of charged-particle $\sum p_{\mathrm{T}}$ (*top row*) and charged multiplicity (*bottom row*) densities against the leading-jet p_{T}, for the inclusive jet (*left column*) and exclusive dijet (*right column*) event selection. The jets are required to have p_{T} of at least 20 GeV, and be within $|y| < 2.8$, whereas the charged particles have at least a p_{T} of 0.5 GeV and $|\eta| < 2.5$. The plots compare the trans-max/min/diff observables to each other and the PYTHIA 6 Perugia 2011 MC model. The *error bands* in the *top plot* show the combined statistical and systematic uncertainty, while the *grey error band* in the *bottom plot* is the envelope of the maximum combined statistical and systematic uncertainty of the trans-max and trans-min regions

In the max/min characterisation of exclusive dijet events, the distinction between the behaviours of the min and max sides is reduced relative to the inclusive jet selection, with either both slightly falling (N_{ch}) or the trans-max observable remaining roughly constant while the trans-min one falls ($\sum p_{\mathrm{T}}$). As in the general transverse-region observables of Fig. 3, this fall-off behaviour is not fully understood, but is consistent with the exclusive dijet cuts excluding events with hard MPI activity, an effect which is expected to be more pronounced in the trans-min region where contamination from hard process radiation is minimised.

The insensitivity of the inclusive jet trans-min region to changes in $p_{\mathrm{T}}^{\mathrm{lead}}$ indicates that UE activity can indeed be modelled as approaching a constant as a function of hard process scale once the scale is hard enough that the proton impact parameters are effectively zero and all collisions are central. However, the observed dependence of the exclusive dijet trans-min observables to changes in hard process scale is clearly worthy of further investigation.

All MC models considered reproduce the qualitative features of the inclusive jet data. However, the PYTHIA models, which have received the most UE tuning attention in recent years, are unexpectedly further from the data than the less flexible and less tuned HERWIG++ and HERWIG+JIMMY models on these observables.

The spread of MC models around the exclusive dijet data is in fact slightly less than for the inclusive jet ones, although the MC models tend not to predict quite as steep

a decrease in UE activity with $p_{\mathrm{T}}^{\mathrm{lead}}$ as in the data. The PYTHIA 6 Perugia 2011 model provides a good combined description of transverse-region $\sum p_{\mathrm{T}}$ and N_{ch} densities, but PYTHIA 8 produces too much transverse-region activity and PYTHIA 6 DW and HERWIG++ undershoot the data. A substantial difference is seen between HERWIG+JIMMY and the combination of HERWIG and JIMMY with ALPGEN matrix elements; the ALPGEN+HERWIG+JIMMY combination is more active in all observables, for both inclusive jet and exclusive dijet selections. It is surprising that this is the case for the exclusive dijet selection, since that is dominated by the $2 \rightarrow 2$ QCD hard process contained in both HERWIG and ALPGEN.

The POWHEG+PYTHIA 6 model is seen to produce slightly lower mean UE activity than standalone PYTHIA 6 Perugia 2011 in both the N_{ch} and $\sum p_{\mathrm{T}}$ density profile observables and for both inclusive jet and exclusive dijet event selections, although the two models produce similar shapes; neither is consistently closer to data than the other, however, and a specialised shower generator tune for use with POWHEG could achieve a better data description.

Finally, it is interesting to compare the trans-diff observables between the inclusive and exclusive jet selections; trans-diff is intended to be most sensitive to additional hard scattering from either MPI or ISR from hard-process, and indeed it may be seen in Fig. 4 to be much flatter for the exclusive dijet topology, as compared to its large increase with $p_{\mathrm{T}}^{\mathrm{lead}}$ for the inclusive distributions. Again, this behaviour is well-modelled by the PYTHIA 6 MC generator, with particularly good numerical agreement for the simulation of trans-diff in the exclusive dijet selection.

8.3 Charged and neutral particle $\sum E_{\mathrm{T}}$ vs. $p_{\mathrm{T}}^{\mathrm{lead}}$

In Fig. 5 the corrected charged and neutral particle $\sum E_{\mathrm{T}}$ density is shown for both the central region (in the top row) and the full η acceptance range (the middle row), for the inclusive jet and exclusive dijet topologies. The trends are broadly similar to those for the track-based observables, and for the central $|\eta|$ range the comparison between the data and MC models is comparable to that seen for the equivalent charged-particle $\sum p_{\mathrm{T}}$ density plots. However, the full acceptance plots show increased disagreement between the MC models and the data; the MC models undershoot the observed level of activity at low $p_{\mathrm{T}}^{\mathrm{lead}}$ values in both the inclusive and exclusive event selections. This discrepancy is notable since all MPI models have to date been tuned to observables measured solely for central rapidities. In the full-acceptance inclusive jet observable, all models except pure HERWIG+JIMMY predict a faster rise of $\sum E_{\mathrm{T}}$ as a function of $p_{\mathrm{T}}^{\mathrm{lead}}$ than seen in the data, although notably most start significantly below the data at low $p_{\mathrm{T}}^{\mathrm{lead}}$.

Finally, the profiles of the ratio $\sum p_{\mathrm{T}}(\mathrm{charged}) / \sum E_{\mathrm{T}}(\mathrm{all})$ in $|\eta| < 2.5$ against $p_{\mathrm{T}}^{\mathrm{lead}}$ are shown in the bottom row of Fig. 5. These observables are mostly flat, and are described well by models other than those using HERWIG+JIMMY parton showering and hadronisation, including the ALPGEN sample. These models lie 10–20 % below the data, indicating a too-low charged fraction resulting from the HERWIG+JIMMY modelling. The ratio nature of this observable means that a large statistical error is seen in the bin around 50 GeV, corresponding to the low-statistics tail of events from the minimum bias trigger before the transition to the jet trigger at $p_{\mathrm{T}}^{\mathrm{lead}} = 60$ GeV.

8.4 Charged-particle mean p_{T} vs. $p_{\mathrm{T}}^{\mathrm{lead}}$ and N_{ch}

In Fig. 6, the distributions of transverse-region charged-particle mean p_{T} against $p_{\mathrm{T}}^{\mathrm{lead}}$ and the transverse region charged-particle multiplicity are shown. No max/min region subdivision is made for the mean p_{T} observables since while there is a clear case for identifying the more and less active sides of an event based on particle multiplicity or momentum flow, the physics interpretation of the transverse side with the higher/lower average particle p_{T} is not as clear as for the pure $\sum p_{\mathrm{T}}$ and N_{ch} observables.

The mean p_{T} vs. $p_{\mathrm{T}}^{\mathrm{lead}}$ profile displays a very different behaviour between the inclusive jet and exclusive dijet event selections; in the inclusive jet case $\langle \text{mean } p_{\mathrm{T}} \rangle$ rises strongly with increasing $p_{\mathrm{T}}^{\mathrm{lead}}$, but when the event selection is restricted to dijet events only, the correlation disappears to give a distribution flat within uncertainties. The roots of this behaviour may be seen in Fig. 3: in the inclusive jet case the N_{ch} profile (the denominator in construction of mean p_{T}) is less sharply rising than $\sum p_{\mathrm{T}}$ (the numerator) as a function of $p_{\mathrm{T}}^{\mathrm{lead}}$, while for the exclusive dijet selection there is less distinction between $\sum p_{\mathrm{T}}$ and N_{ch}, leading to the flat ratio. Based on previous conclusions about the nature of the contributions to the trans-max and trans-min components of the $\sum p_{\mathrm{T}}$ and N_{ch} density vs. $p_{\mathrm{T}}^{\mathrm{lead}}$ profiles, this distinction between inclusive and exclusive mean p_{T} behaviours implies that it is the high-p_{T} tails of UE particle production (which are effectively removed by the dijet selection) that are responsible for the slight increase in mean p_{T} in the inclusive jet selection.

For both the inclusive jet and exclusive dijet selections, the transverse-region mean p_{T} as a function of $p_{\mathrm{T}}^{\mathrm{lead}}$ is well-described by the MC models—within 10 % of the data. This is as expected, since the descriptions of the related transverse-region charged-particle $\sum p_{\mathrm{T}}$ and multiplicity densities were described to similar levels of precision.

The $\langle \text{mean } p_{\mathrm{T}} \rangle$ vs. N_{ch} plots follow the pattern established by previous experiments, with mean particle p_{T} increasing as a function of the number of charged particles. This observable is particularly well described by HERWIG++,

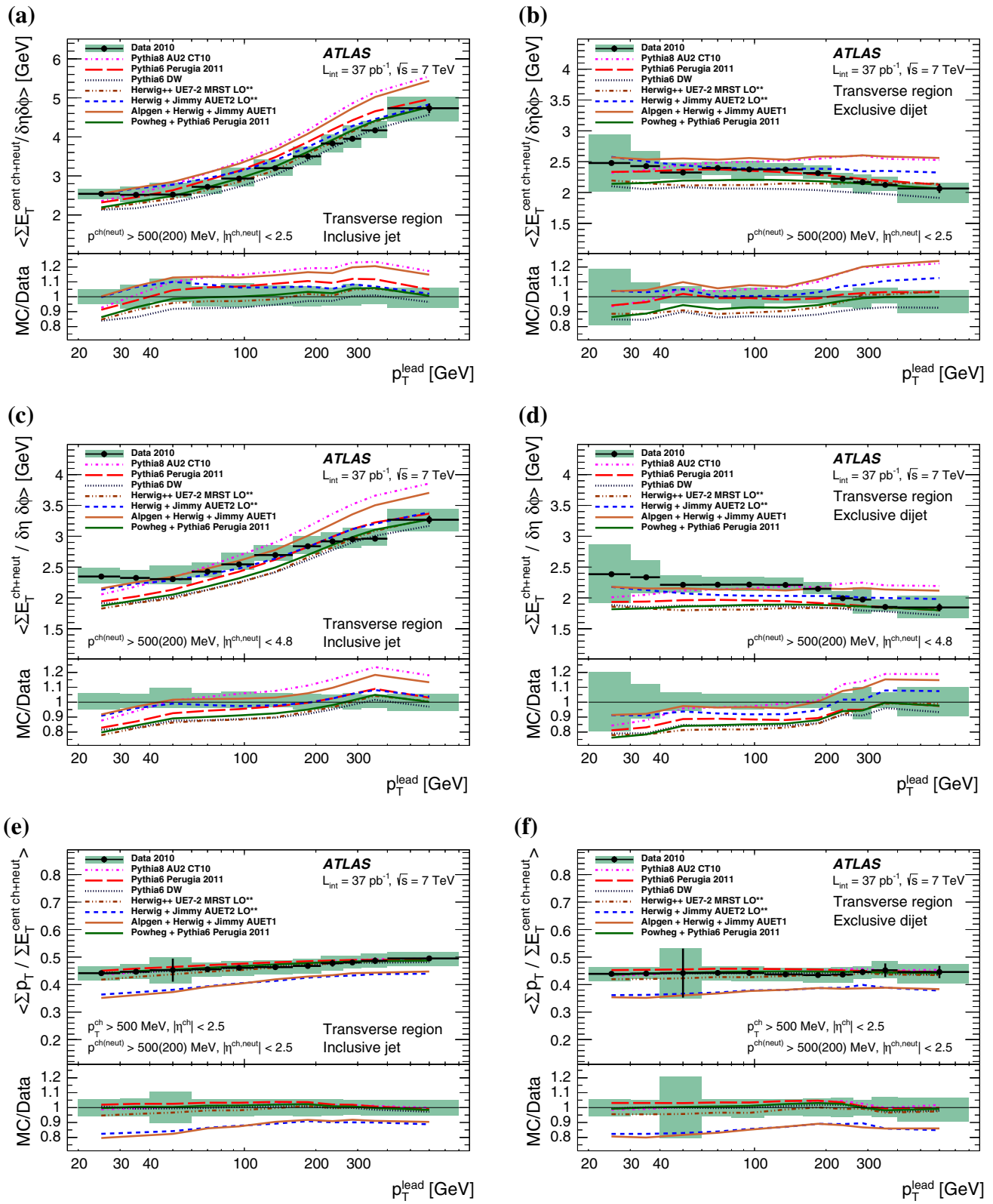

Fig. 5 Transverse region profiles of $\sum E_{\mathrm{T}}$ of the neutral and charged particles for the inclusive (*left*) and exclusive dijet (*right*) selection against the leading-jet p_{T} for the central region (*top row*) and the full acceptance region (*middle row*). The *bottom row* shows transverse region profiles of $\langle \sum p_{\mathrm{T}}(\mathrm{charged}) / \sum E_{\mathrm{T}}(\mathrm{all}) \rangle$ for the inclusive (*left*) and exclusive dijet (*right*) selection constructed from charged and neutral particles against the leading-jet p_{T}. The jets are required to have p_{T} of at least 20 GeV, and be within $|y| < 2.8$. The *error bars* show the statistical uncertainty while the *shaded area* shows the combined statistical and systematic uncertainty

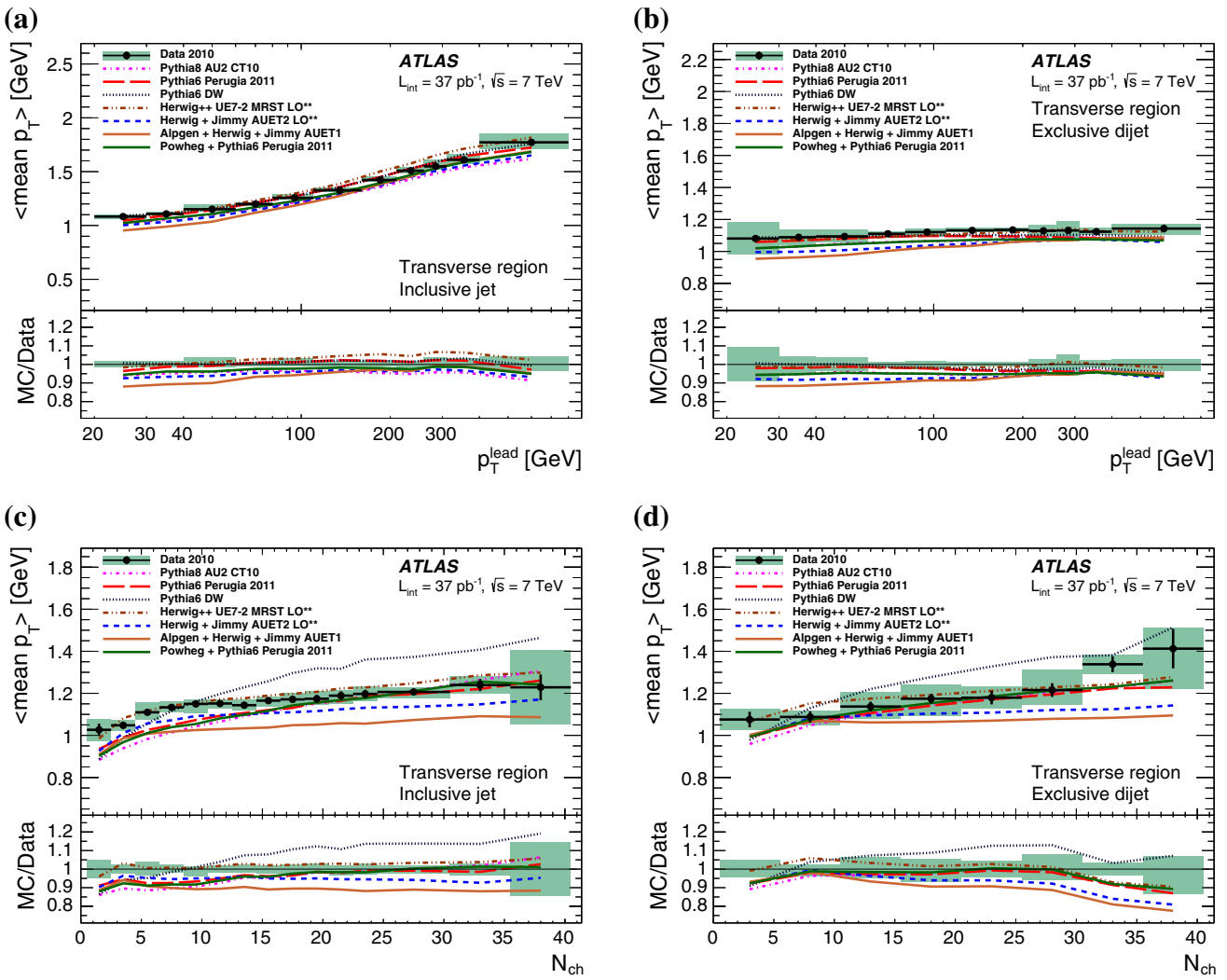

Fig. 6 Transverse region profiles of the mean p_{T} of charged particles for the inclusive (*left*) and exclusive dijet (*right*) selection against the leading-jet p_{T} (*top row*) and charged-particle multiplicity (*bottom row*). The jets are required to have p_{T} of at least 20 GeV and to be within $|y| < 2.8$, whereas the charged particles have at least a p_{T} of 0.5 GeV and $|\eta| < 2.5$. The *error bars* show the statistical uncertainty while the *shaded area* shows the combined statistical and systematic uncertainty

which is the only generator to give a good description of the observable for inclusive jet events with fewer than 17 particles in the transverse region. The bulk of the MC models considered give predictions consistent with the data for the exclusive dijet event selection. The main outliers are PYTHIA 6 Tune DW, which overshoots the data in both selections for events with more than about 10 charged particles, and HERWIG+JIMMY both standalone and in combination with ALPGEN, which significantly undershoot. The ALPGEN+HERWIG+JIMMY configuration, which uses the older AUET1 tune of JIMMY, undershoots the data by the greatest amount.

An underestimation of $\langle \text{mean } p_{\mathrm{T}} \rangle$ vs. N_{ch} data are not unexpected from the JIMMY model, as it contains no colour reconnection mechanism to redistribute momentum in high-multiplicity events [50]. The newer AUET2 tune of HERWIG+JIMMY manages to do slightly better than AUET1 as used with ALPGEN, but remains significantly outside the experimental uncertainties. By comparison HERWIG++, which has a similar MPI implementation but does use a colour reconnection model, agrees well with the data.

Finally, the ATLAS tunes of both PYTHIA 6 and PYTHIA 8 are seen to undershoot the data for low N_{ch}, particularly in the inclusive jet sample, but describe the $\langle \text{mean } p_{\mathrm{T}} \rangle$ of higher-multiplicity events well for both event selections. As both these tunes incorporated the equivalent of this observable in the ATLAS leading charged-particle UE analysis [3], the flaws in their data description seen here are unexpected, and use of these data in future tunes may substantially change the MPI model parameters.

9 Summary and conclusions

ATLAS measurements sensitive to the underlying event in 37 pb^{-1} of 7 TeV proton–proton collisions at the LHC have been presented, using observables constructed with respect to QCD jets with p_{T} up to 800 GeV. Inclusive jet and exclusive dijet event topologies have been considered separately, and measures of UE activity azimuthally transverse to the leading jet computed using both charged-particle tracks and all-particle clusters of energy deposited in the calorimeters. The observables have been further subdivided into trans-max and trans-min regions on an event-by-event basis depending on which side of the event had more activity: this subdivision provides additional discriminating power between the component processes of the UE.

The most notable features of the observables presented in this paper are as follows:

- Rising levels of transverse-region activity as a function of leading-jet p_{T}, as previously observed in UE studies, are seen in the inclusive jets event selection, with the exception of the inclusive trans-min region.
- Application of an exclusive dijet event selection requirement removes this feature, producing instead transverse-region activity measures which are constant or which slightly decrease with increasing leading-jet p_{T}. This decrease in activity is not obviously expected from a simple picture of the underlying event and is deserving of further investigation.
- The behaviour of underlying event particle flow observables in exclusive dijet topologies indicates that pure MPI activity can largely be modelled as independent of hard process scale, provided that scale is hard enough that all proton–proton interactions are central.

These observables have been compared to a number of MC models, using several tunes of commonly used underlying event models. The data are broadly consistent with the predictions of the multiple partonic scattering paradigm, although indicative of several areas where MPI parameter tuning may improve MC data description in further LHC studies. Again, several key features are of note:

- MC models in general provide a good qualitative description of the data behaviour, but there are some significant discrepancies. The HERWIG+JIMMY and HERWIG++ generators currently describe inclusive jet UE observables slightly better than the PYTHIA family, but the PYTHIA 6 tunes perform better on UE in exclusive dijet topologies.
- HERWIG++ shows significant improvements over the HERWIG+JIMMY configuration. However, PYTHIA 8 is seen to produce too much UE activity, and will require retuning of underlying event parameters to perform comparably to its FORTRAN predecessor.
- For the exclusive dijet event selection, the decrease of transverse region activity in data is stronger than seen in the available MC models, indicating that there are aspects of the UE yet to be understood and incorporated into MC models.
- Full $|\eta|$-range cluster observables show larger deviations from MC predictions than in the central region, indicating a region of phase space in which all MC models can be improved.

These data provide a detailed measurement of the pp underlying event in QCD jet events, with momentum sums and charged-particle multiplicities measured both as distributions and as profiles of their means as functions of the hard process scale. The separate evaluations of the observables for inclusive jet vs. exclusive dijet event selections, charged-particle vs. all-particle energy flows, central vs. full η acceptance, and transverse/trans-max/trans-min categories enable more specific MC model comparisons than possible with preceding public data. These measurements are hence expected to play a significant role in the future development and tuning of MC models of the underlying event.

Acknowledgments We thank CERN for the very successful operation of the LHC, as well as the support staff from our institutions without whom ATLAS could not be operated efficiently. We acknowledge the support of ANPCyT, Argentina; YerPhI, Armenia; ARC, Australia; BMWF and FWF, Austria; ANAS, Azerbaijan; SSTC, Belarus; CNPq and FAPESP, Brazil; NSERC, NRC and CFI, Canada; CERN; CONICYT, Chile; CAS, MOST and NSFC, China; COLCIENCIAS, Colombia; MSMT CR, MPO CR and VSC CR, Czech Republic; DNRF, DNSRC and Lundbeck Foundation, Denmark; EPLANET, ERC and NSRF, European Union; IN2P3-CNRS, CEA-DSM/IRFU, France; GNSF, Georgia; BMBF, DFG, HGF, MPG and AvH Foundation, Germany; GSRT and NSRF, Greece; ISF, MINERVA, GIF, I-CORE and Benoziyo Center, Israel; INFN, Italy; MEXT and JSPS, Japan; CNRST, Morocco; FOM and NWO, Netherlands; BRF and RCN, Norway; MNiSW and NCN, Poland; GRICES and FCT, Portugal; MNE/IFA, Romania; MES of Russia and ROSATOM, Russian Federation; JINR; MSTD, Serbia; MSSR, Slovakia; ARRS and MIZŠ, Slovenia; DST/NRF, South Africa; MINECO, Spain; SRC and Wallenberg Foundation, Sweden; SER, SNSF and Cantons of Bern and Geneva, Switzerland; NSC, Taiwan; TAEK, Turkey; STFC, the Royal Society and Leverhulme Trust, United Kingdom; DOE and NSF, United States of America. The crucial computing support from all WLCG partners is acknowledged gratefully, in particular from CERN and the ATLAS Tier-1 facilities at TRIUMF (Canada), NDGF (Denmark, Norway, Sweden), CC-IN2P3 (France), KIT/GridKA (Germany), INFN-CNAF (Italy), NL-T1 (Netherlands), PIC (Spain), ASGC (Taiwan), RAL (UK) and BNL (USA) and in the Tier-2 facilities worldwide.

References

1. CDF Collaboration, D. Acosta et al., The underlying event in hard interactions at the Tevatron $\bar{p}p$ collider. Phys. Rev. D **70**, 072002 (2004). arXiv:hep-ex/0404004
2. CDF Collaboration, T. Aaltonen et al., Studying the underlying event in Drell–Yan and high transverse momentum jet production at the Tevatron. Phys. Rev. D **82**, 034001 (2010). arXiv:1003.3146 [hep-ex]
3. ATLAS Collaboration, Measurement of underlying event characteristics using charged particles in pp collisions at $\sqrt{s} = 900$ GeV and 7 TeV with the ATLAS detector. Phys. Rev. D **83**, 112001 (2011). arXiv:1012.0791 [hep-ex]
4. ATLAS Collaboration, Measurements of underlying-event properties using neutral and charged particles in pp collisions at 900 GeV and 7 TeV with the ATLAS detector at the LHC. Eur. Phys. J. C **71**, 1636 (2011). arXiv:1103.1816 [hep-ex]
5. ATLAS Collaboration, Underlying event characteristics and their dependence on jet size of charged-particle jet events in pp collisions at $\sqrt{s} = 7$ TeV with the ATLAS detector. Phys. Rev. D **86**, 072004 (2012). arXiv:1208.0563 [hep-ex]
6. ATLAS Collaboration, Measurements of the pseudorapidity dependence of the total transverse energy in proton–proton collisions at $\sqrt{s} = 7$ TeV with ATLAS. J. High Energy Phys. **1211**, 033 (2012). arXiv:1208.6256 [hep-ex]
7. ALICE Collaboration, Underlying event measurements in pp collisions at $\sqrt{s} = 0.9$ and 7 TeV with the ALICE experiment at the LHC. J. High Energy Phys. **1207**, 116 (2012). arXiv:1112.2082 [hep-ex]
8. CMS Collaboration, Measurement of the underlying event activity in proton–proton collisions at 0.9 TeV. Eur. Phys. J. C **70**, 555–572 (2010). arXiv:1006.2083 [hep-ex]
9. CMS Collaboration, Measurement of the underlying event in the Drell–Yan process in proton–proton collisions at $\sqrt{s} = 7$ TeV. Eur. Phys. J. C **72**, 2080 (2012). doi:10.1140/epjc/s10052-012-2080-4. arXiv:1204.1411 [hep-ex]
10. ATLAS Collaboration, The ATLAS experiment at the CERN large hadron collider. JINST **3**, S08003 (2008)
11. W. Lampl et al., Calorimeter clustering algorithms: description and performance. ATL-LARG-PUB-2008-002 (2008)
12. M. Cacciari, G. Salam, G. Soyez, The anti-k_t jet clustering algorithm. J. High Energy Phys. **04**, 063 (2008). arXiv:0802.1189 [hep-ph]
13. G. Marchesini, B. Webber, Associated transverse energy in hadronic jet production. Phys. Rev. D **38**, 3419 (1988)
14. J. Pumplin, Hard underlying event correction to inclusive jet cross sections. Phys. Rev. D **57**(9), 5787–5792 (1998). arXiv:hep-ph/9708464
15. ATLAS Collaboration, Measurement of multi-jet cross sections in proton–proton collisions at a 7 TeV center-of-mass energy. Eur. Phys. J. C **71**, 1763 (2011). arXiv:1107.2092 [hep-ex]
16. T. Sjostrand, S. Mrenna, P. Skands, PYTHIA 6.4 physics and manual. J. High Energy Phys. **05**, 026 (2006). arXiv:hep-ph/0603175
17. T. Sjostrand, S. Mrenna, P. Skands, A brief introduction to PYTHIA 8.1. Comput. Phys. Commun. **178**, 852–867 (2008). arXiv:0710.3820 [hep-ph]
18. S. Gieseke et al., Herwig++ 2.5 release note. arXiv:1102.1672 [hep-ph]
19. V. Khoze, F. Krauss, A. Martin, M. Ryskin, K. Zapp, Diffraction and correlations at the LHC: definitions and observables. Eur. Phys. J. C **69**, 85–93 (2010). arXiv:1005.4839 [hep-ph]
20. M.H. Seymour, A. Siodmok, Constraining MPI models using σ_{eff} and recent Tevatron and LHC underlying event data. J. High Energy Phys. **1310**, 113 (2013). arXiv:1307.5015 [hep-ph]
21. G. Corcella, I.G. Knowles, G. Marchesini, S. Moretti, K. Odagiri et al., HERWIG 6: an event generator for hadron emission reactions with interfering gluons (including supersymmetric processes). JHEP. **0101**, 010 (2001). doi:10.1088/1126-6708/2001/01/010. arXiv:hep-ph/0011363
22. M. Bahr et al., Herwig++ physics and manual. Eur. Phys. J. C **58**, 639–707 (2008). arXiv:0803.0883 [hep-ph]
23. M.L. Mangano, M. Moretti, F. Piccinini, R. Pittau, A.D. Polosa, ALPGEN, a generator for hard multiparton processes in hadronic collisions. J. High Energy Phys. **0307**, 001 (2003). arXiv:hep-ph/0206293
24. S. Alioli, K. Hamilton, P. Nason, C. Oleari, E. Re, Jet pair production in POWHEG. J. High Energy Phys. **1104**, 081 (2011). arXiv:1012.3380 [hep-ph]
25. J.M. Butterworth, J.R. Forshaw, M.H. Seymour, Multiparton interactions in photoproduction at HERA. Z. Phys. C **72**, 637–646 (1996). arXiv:hep-ph/9601371
26. ATLAS Collaboration, Measurement of the inclusive jet cross section in pp collisions at $\sqrt{s} = 2.76$ TeV and comparison to the inclusive jet cross section at $\sqrt{s} = 7$ TeV using the ATLAS detector. Eur. Phys. J. C **73**, 2509 (2013). arXiv:1304.4739 [hep-ex]
27. P. Nason, C. Oleari, Generation cuts and Born suppression in POWHEG. arXiv:1303.3922 [hep-ph]
28. ATLAS Collaboration, Summary of ATLAS PYTHIA 8 tunes. ATL-PHYS-PUB-2012-003 (2012)
29. H.-L. Lai, M. Guzzi, J. Huston, Z. Li, P.M. Nadolsky et al., New parton distributions for collider physics. Phys. Rev. D **82**, 074024 (2010). doi:10.1103/PhysRevD.82.074024. arXiv:1007.2241 [hep-ph]
30. P.Z. Skands, Tuning Monte Carlo generators: the Perugia tunes. Phys. Rev. D **82**, 074018 (2010). arXiv:1005.3457 [hep-ph]. Perugia 2011 tunes described in arXiv update
31. CTEQ Collaboration, H. Lai et al., Global QCD analysis of parton structure of the nucleon: CTEQ5 parton distributions. Eur. Phys. J. C **12**, 375–392 (2000). arXiv:hep-ph/9903282
32. CDF Collaboration, R. Field, CDF Run II Monte-Carlo tunes. FERMILAB-PUB-06-408-E
33. S. Gieseke, C. Rohr, A. Siodmok, Multiple partonic interaction developments in Herwig++. arXiv:1110.2675 [hep-ph]
34. A. Sherstnev, R. Thorne, Different PDF approximations useful for LO Monte Carlo generators. arXiv:0807.2132 [hep-ph]
35. ATLAS Collaboration, First tuning of HERWIG + JIMMY to ATLAS data. ATL-PHYS-PUB-2010-014 (2010)
36. J. Pumplin, D. Stump, J. Huston, H. Lai, P.M. Nadolsky et al., New generation of parton distributions with uncertainties from global QCD analysis. J. High Energy Phys. **0207**, 012 (2002). arXiv:hep-ph/0201195
37. ATLAS Collaboration, New ATLAS event generator tunes to 2010 data. ATL-PHYS-PUB-2011-008 (2011)
38. A. Sherstnev, R.S. Thorne, Parton distributions for LO generators. Eur. Phys. J. C **55**, 553–575 (2008). arXiv:0711.2473 [hep-ph]
39. HERWIG++ Collaboration, HERWIG++ minimum-bias and underlying-event tunes. https://herwig.hepforge.org/trac/wiki/MB_UE_tunes
40. ATLAS Collaboration, Charged-particle multiplicities in pp interactions measured with the ATLAS detector at the LHC. New J. Phys. **13**, 053033 (2011). arXiv:1012.5104 [hep-ex]
41. ATLAS Collaboration, The ATLAS simulation infrastructure. Eur. Phys. J. C **70**, 823–874 (2010). arXiv:1005.4568 [physics.ins-det]
42. Geant4 Collaboration, S. Agostinelli et al., Geant4: a simulation toolkit. Nucl. Instrum. Methods A **506**, 250–303 (2003)
43. ATLAS Collaboration, ATLAS tunes of PYTHIA 6 and PYTHIA 8 for MC11. ATL-PHYS-PUB-2011-009 (2011)

44. ATLAS Collaboration, Improved luminosity determination in pp collisions at $\sqrt{s} = 7$ TeV using the ATLAS detector at the LHC. Eur. Phys. J. C **73**, 2518 (2013). arXiv:1302.4393 [hep-ex]
45. ATLAS Collaboration, Measurement of inclusive jet and dijet production in pp collisions at $\sqrt{s} = 7$ TeV using the ATLAS detector. Phys. Rev. D **86**, 014022 (2012). arXiv:1112.6297 [hep-ex]
46. ATLAS Collaboration, Hadronic calibration of the ATLAS liquid argon end-cap calorimeter in the pseudorapidity region in beam tests. Nucl. Instrum. Methods A **531**(3), 481–514 (2004). arXiv:physics/0407009
47. G. D'Agostini, A multidimensional unfolding method based on Bayes' theorem. Nucl. Instrum. Methods A **362**, 487–498 (1995)
48. B. Wynne, Imagiro: an implementation of Bayesian iterative unfolding for high-energy physics. arXiv:1203.4981 [physics.data-an]
49. ATLAS Collaboration, Jet energy measurement with the ATLAS detector in proton-proton collisions at $\sqrt{s} = 7$ TeV. Eur. Phys. J. C **73**, 2304 (2011). arXiv:1112.6426 [hep-ex]
50. A. Buckley, Soft QCD in ATLAS: measurements and modelling of multi-parton interactions. Acta Phys. Polon. B **42**, 2669–2696 (2011). arXiv:1112.5477 [hep-ph]

The ATLAS Collaboration

G. Aad[84], T. Abajyan[21], B. Abbott[112], J. Abdallah[152], S. Abdel Khalek[116], O. Abdinov[11], R. Aben[106], B. Abi[113], M. Abolins[89], O. S. AbouZeid[159], H. Abramowicz[154], H. Abreu[137], Y. Abulaiti[147a,147b], B. S. Acharya[165a,165b,a], L. Adamczyk[38a], D. L. Adams[25], T. N. Addy[56], J. Adelman[177], S. Adomeit[99], T. Adye[130], T. Agatonovic-Jovin[13b], J. A. Aguilar-Saavedra[125a,125f], M. Agustoni[17], S. P. Ahlen[22], F. Ahmadov[64,b], G. Aielli[134a,134b], T. P. A. Åkesson[80], G. Akimoto[156], A. V. Akimov[95], J. Albert[170], S. Albrand[55], M. J. Alconada Verzini[70], M. Aleksa[30], I. N. Aleksandrov[64], C. Alexa[26a], G. Alexander[154], G. Alexandre[49], T. Alexopoulos[10], M. Alhroob[165a,165c], G. Alimonti[90a], L. Alio[84], J. Alison[31], B. M. M. Allbrooke[18], L. J. Allison[71], P. P. Allport[73], S. E. Allwood-Spiers[53], J. Almond[83], A. Aloisio[103a,103b], R. Alon[173], A. Alonso[36], F. Alonso[70], C. Alpigiani[75], A. Altheimer[35], B. Alvarez Gonzalez[89], M. G. Alviggi[103a,103b], K. Amako[65], Y. Amaral Coutinho[24a], C. Amelung[23], D. Amidei[88], V. V. Ammosov[129,*], S. P. Amor Dos Santos[125a,125c], A. Amorim[125a,125b], S. Amoroso[48], N. Amram[154], G. Amundsen[23], C. Anastopoulos[140], L. S. Ancu[17], N. Andari[30], T. Andeen[35], C. F. Anders[58b], G. Anders[30], K. J. Anderson[31], A. Andreazza[90a,90b], V. Andrei[58a], X. S. Anduaga[70], S. Angelidakis[9], P. Anger[44], A. Angerami[35], F. Anghinolfi[30], A. V. Anisenkov[108], N. Anjos[125a], A. Annovi[47], A. Antonaki[9], M. Antonelli[47], A. Antonov[97], J. Antos[145b], F. Anulli[133a], M. Aoki[65], L. Aperio Bella[18], R. Apolle[119,c], G. Arabidze[89], I. Aracena[144], Y. Arai[65], J. P. Araque[125a], A. T. H. Arce[45], J-F. Arguin[94], S. Argyropoulos[42], M. Arik[19a], A. J. Armbruster[30], O. Arnaez[82], V. Arnal[81], O. Arslan[21], A. Artamonov[96], G. Artoni[23], S. Asai[156], N. Asbah[94], A. Ashkenazi[154], S. Ask[28], B. Åsman[147a,147b], L. Asquith[6], K. Assamagan[25], R. Astalos[145a], M. Atkinson[166], N. B. Atlay[142], B. Auerbach[6], E. Auge[116], K. Augsten[127], M. Aurousseau[146b], G. Avolio[30], G. Azuelos[94,d], Y. Azuma[156], M. A. Baak[30], C. Bacci[135a,135b], A. M. Bach[15], H. Bachacou[137], K. Bachas[155], M. Backes[30], M. Backhaus[30], J. Backus Mayes[144], E. Badescu[26a], P. Bagiacchi[133a,133b], P. Bagnaia[133a,133b], Y. Bai[33a], D. C. Bailey[159], T. Bain[35], J. T. Baines[130], O. K. Baker[177], S. Baker[77], P. Balek[128], F. Balli[137], E. Banas[39], Sw. Banerjee[174], A. Bangert[151], A. A. E. Bannoura[176], V. Bansal[170], H. S. Bansil[18], L. Barak[173], S. P. Baranov[95], T. Barber[48], E. L. Barberio[87], D. Barberis[50a,50b], M. Barbero[84], T. Barillari[100], M. Barisonzi[176], T. Barklow[144], N. Barlow[28], B. M. Barnett[130], R. M. Barnett[15], Z. Barnovska[5], A. Baroncelli[135a], G. Barone[49], A. J. Barr[119], F. Barreiro[81], J. Barreiro Guimarães da Costa[57], R. Bartoldus[144], A. E. Barton[71], P. Bartos[145a], V. Bartsch[150], A. Bassalat[116], A. Basye[166], R. L. Bates[53], L. Batkova[145a], J. R. Batley[28], M. Battistin[30], F. Bauer[137], H. S. Bawa[144,e], T. Beau[79], P. H. Beauchemin[162], R. Beccherle[123a,123b], P. Bechtle[21], H. P. Beck[17], K. Becker[176], S. Becker[99], M. Beckingham[139], C. Becot[116], A. J. Beddall[19c], A. Beddall[19c], S. Bedikian[177], V. A. Bednyakov[64], C. P. Bee[149], L. J. Beemster[106], T. A. Beermann[176], M. Begel[25], K. Behr[119], C. Belanger-Champagne[86], P. J. Bell[49], W. H. Bell[49], G. Bella[154], L. Bellagamba[20a], A. Bellerive[29], M. Bellomo[85], A. Belloni[57], K. Belotskiy[97], O. Beltramello[30], O. Benary[154], D. Benchekroun[136a], K. Bendtz[147a,147b], N. Benekos[166], Y. Benhammou[154], E. Benhar Noccioli[49], J. A. Benitez Garcia[160b], D. P. Benjamin[45], J. R. Bensinger[23], K. Benslama[131], S. Bentvelsen[106], D. Berge[106], E. Bergeaas Kuutmann[16], N. Berger[5], F. Berghaus[170], E. Berglund[106], J. Beringer[15], C. Bernard[22], P. Bernat[77], C. Bernius[78], F. U. Bernlochner[170], T. Berry[76], P. Berta[128], C. Bertella[84], F. Bertolucci[123a,123b], M. I. Besana[90a], G. J. Besjes[105], O. Bessidskaia[147a,147b], N. Besson[137], C. Betancourt[48], S. Bethke[100], W. Bhimji[46], R. M. Bianchi[124], L. Bianchini[23], M. Bianco[30], O. Biebel[99], S. P. Bieniek[77], K. Bierwagen[54], J. Biesiada[15], M. Biglietti[135a], J. Bilbao De Mendizabal[49], H. Bilokon[47], M. Bindi[54], S. Binet[116], A. Bingul[19c], C. Bini[133a,133b], C. W. Black[151], J. E. Black[144], K. M. Black[22], D. Blackburn[139], R. E. Blair[6], J.-B. Blanchard[137], T. Blazek[145a], I. Bloch[42], C. Blocker[23], W. Blum[82,*], U. Blumenschein[54], G. J. Bobbink[106], V. S. Bobrovnikov[108], S. S. Bocchetta[80], A. Bocci[45], C. R. Boddy[119], M. Boehler[48], J. Boek[176], T. T. Boek[176], J. A. Bogaerts[30], A. G. Bogdanchikov[108], A. Bogouch[91,*], C. Bohm[147a], J. Bohm[126], V. Boisvert[76], T. Bold[38a], V. Boldea[26a], A. S. Boldyrev[98], N. M. Bolnet[137], M. Bomben[79], M. Bona[75], M. Boonekamp[137], A. Borisov[129], G. Borissov[71], M. Borri[83], S. Borroni[42], J. Bortfeldt[99], V. Bortolotto[135a,135b], K. Bos[106], D. Boscherini[20a], M. Bosman[12], H. Boterenbrood[106], J. Boudreau[124], J. Bouffard[2], E. V. Bouhova-Thacker[71], D. Boumediene[34],

C. Bourdarios[116], N. Bousson[113], S. Boutouil[136d], A. Boveia[31], J. Boyd[30], I. R. Boyko[64], I. Bozovic-Jelisavcic[13b], J. Bracinik[18], P. Branchini[135a], A. Brandt[8], G. Brandt[15], O. Brandt[58a], U. Bratzler[157], B. Brau[85], J. E. Brau[115], H. M. Braun[176,*], S. F. Brazzale[165a,165c], B. Brelier[159], K. Brendlinger[121], A. J. Brennan[87], R. Brenner[167], S. Bressler[173], K. Bristow[146c], T. M. Bristow[46], D. Britton[53], F. M. Brochu[28], I. Brock[21], R. Brock[89], C. Bromberg[89], J. Bronner[100], G. Brooijmans[35], T. Brooks[76], W. K. Brooks[32b], J. Brosamer[15], E. Brost[115], G. Brown[83], J. Brown[55], P. A. Bruckman de Renstrom[39], D. Bruncko[145b], R. Bruneliere[48], S. Brunet[60], A. Bruni[20a], G. Bruni[20a], M. Bruschi[20a], L. Bryngemark[80], T. Buanes[14], Q. Buat[143], F. Bucci[49], P. Buchholz[142], R. M. Buckingham[119], A. G. Buckley[53], S. I. Buda[26a], I. A. Budagov[64], F. Buehrer[48], L. Bugge[118], M. K. Bugge[118], O. Bulekov[97], A. C. Bundock[73], H. Burckhart[30], S. Burdin[73], B. Burghgrave[107], S. Burke[130], I. Burmeister[43], E. Busato[34], V. Büscher[82], P. Bussey[53], C. P. Buszello[167], B. Butler[57], J. M. Butler[22], A. I. Butt[3], C. M. Buttar[53], J. M. Butterworth[77], P. Butti[106], W. Buttinger[28], A. Buzatu[53], M. Byszewski[10], S. Cabrera Urbán[168], D. Caforio[20a,20b], O. Cakir[4a], P. Calafiura[15], G. Calderini[79], P. Calfayan[99], R. Calkins[107], L. P. Caloba[24a], D. Calvet[34], S. Calvet[34], R. Camacho Toro[49], S. Camarda[42], D. Cameron[118], L. M. Caminada[15], R. Caminal Armadans[12], S. Campana[30], M. Campanelli[77], A. Campoverde[149], V. Canale[103a,103b], A. Canepa[160a], J. Cantero[81], R. Cantrill[76], T. Cao[40], M. D. M. Capeans Garrido[30], I. Caprini[26a], M. Caprini[26a], M. Capua[37a,37b], R. Caputo[82], R. Cardarelli[134a], T. Carli[30], G. Carlino[103a], L. Carminati[90a,90b], S. Caron[105], E. Carquin[32a], G. D. Carrillo-Montoya[146c], J. R. Carter[28], J. Carvalho[125a,125c], D. Casadei[77], M. P. Casado[12], E. Castaneda-Miranda[146b], A. Castelli[106], V. Castillo Gimenez[168], N. F. Castro[125a], P. Catastini[57], A. Catinaccio[30], J. R. Catmore[71], A. Cattai[30], G. Cattani[134a,134b], S. Caughron[89], V. Cavaliere[166], D. Cavalli[90a], M. Cavalli-Sforza[12], V. Cavasinni[123a,123b], F. Ceradini[135a,135b], B. Cerio[45], K. Cerny[128], A. S. Cerqueira[24b], A. Cerri[150], L. Cerrito[75], F. Cerutti[15], M. Cerv[30], A. Cervelli[17], S. A. Cetin[19b], A. Chafaq[136a], D. Chakraborty[107], I. Chalupkova[128], K. Chan[3], P. Chang[166], B. Chapleau[86], J. D. Chapman[28], D. Charfeddine[116], D. G. Charlton[18], C. C. Chau[159], C. A. Chavez Barajas[150], S. Cheatham[86], A. Chegwidden[89], S. Chekanov[6], S. V. Chekulaev[160a], G. A. Chelkov[64,f], M. A. Chelstowska[88], C. Chen[63], H. Chen[25], K. Chen[149], L. Chen[33d,g], S. Chen[33c], X. Chen[146c], Y. Chen[35], H. C. Cheng[88], Y. Cheng[31], A. Cheplakov[64], R. Cherkaoui El Moursli[136e], V. Chernyatin[25,*], E. Cheu[7], L. Chevalier[137], V. Chiarella[47], G. Chiefari[103a,103b], J. T. Childers[6], A. Chilingarov[71], G. Chiodini[72a], A. S. Chisholm[18], R. T. Chislett[77], A. Chitan[26a], M. V. Chizhov[64], S. Chouridou[9], B. K. B. Chow[99], I. A. Christidi[77], D. Chromek-Burckhart[30], M. L. Chu[152], J. Chudoba[126], L. Chytka[114], G. Ciapetti[133a,133b], A. K. Ciftci[4a], R. Ciftci[4a], D. Cinca[62], V. Cindro[74], A. Ciocio[15], P. Cirkovic[13b], Z. H. Citron[173], M. Citterio[90a], M. Ciubancan[26a], A. Clark[49], P. J. Clark[46], R. N. Clarke[15], W. Cleland[124], J. C. Clemens[84], B. Clement[55], C. Clement[147a,147b], Y. Coadou[84], M. Cobal[165a,165c], A. Coccaro[139], J. Cochran[63], L. Coffey[23], J. G. Cogan[144], J. Coggeshall[166], B. Cole[35], S. Cole[107], A. P. Colijn[106], C. Collins-Tooth[53], J. Collot[55], T. Colombo[58c], G. Colon[85], G. Compostella[100], P. Conde Muiño[125a,125b], E. Coniavitis[167], M. C. Conidi[12], S. H. Connell[146b], I. A. Connelly[76], S. M. Consonni[90a,90b], V. Consorti[48], S. Constantinescu[26a], C. Conta[120a,120b], G. Conti[57], F. Conventi[103a,h], M. Cooke[15], B. D. Cooper[77], A. M. Cooper-Sarkar[119], N. J. Cooper-Smith[76], K. Copic[15], T. Cornelissen[176], M. Corradi[20a], F. Corriveau[86,i], A. Corso-Radu[164], A. Cortes-Gonzalez[12], G. Cortiana[100], G. Costa[90a], M. J. Costa[168], D. Costanzo[140], D. Côté[8], G. Cottin[28], G. Cowan[76], B. E. Cox[83], K. Cranmer[109], G. Cree[29], S. Crépé-Renaudin[55], F. Crescioli[79], M. Crispin Ortuzar[119], M. Cristinziani[21], G. Crosetti[37a,37b], C.-M. Cuciuc[26a], T. Cuhadar Donszelmann[140], J. Cummings[177], M. Curatolo[47], C. Cuthbert[151], H. Czirr[142], P. Czodrowski[3], Z. Czyczula[177], S. D'Auria[53], M. D'Onofrio[73], M. J. Da Cunha Sargedas De Sousa[125a,125b], C. Da Via[83], W. Dabrowski[38a], A. Dafinca[119], T. Dai[88], O. Dale[14], F. Dallaire[94], C. Dallapiccola[85], M. Dam[36], A. C. Daniells[18], M. Dano Hoffmann[137], V. Dao[105], G. Darbo[50a], G. L. Darlea[26c], S. Darmora[8], J. A. Dassoulas[42], W. Davey[21], C. David[170], T. Davidek[128], E. Davies[119,c], M. Davies[94], O. Davignon[79], A. R. Davison[77], P. Davison[77], Y. Davygora[58a], E. Dawe[143], I. Dawson[140], R. K. Daya-Ishmukhametova[23], K. De[8], R. de Asmundis[103a], S. De Castro[20a,20b], S. De Cecco[79], J. de Graat[99], N. De Groot[105], P. de Jong[106], C. De La Taille[116], H. De la Torre[81], F. De Lorenzi[63], L. De Nooij[106], D. De Pedis[133a], A. De Salvo[133a], U. De Sanctis[165a,165c], A. De Santo[150], J. B. De Vivie De Regie[116], G. De Zorzi[133a,133b], W. J. Dearnaley[71], R. Debbe[25], C. Debenedetti[46], B. Dechenaux[55], D. V. Dedovich[64], J. Degenhardt[121], I. Deigaard[106], J. Del Peso[81], T. Del Prete[123a,123b], F. Deliot[137], M. Deliyergiyev[74], A. Dell'Acqua[30], L. Dell'Asta[22], M. Dell'Orso[123a,123b], M. Della Pietra[103a,h], D. della Volpe[49], M. Delmastro[5], P. A. Delsart[55], C. Deluca[106], S. Demers[177], M. Demichev[64], A. Demilly[79], S. P. Denisov[129], D. Derendarz[39], J. E. Derkaoui[136d], F. Derue[79], P. Dervan[73], K. Desch[21], C. Deterre[42], P. O. Deviveiros[106], A. Dewhurst[130], S. Dhaliwal[106], A. Di Ciaccio[134a,134b], L. Di Ciaccio[5], A. Di Domenico[133a,133b], C. Di Donato[103a,103b], A. Di Girolamo[30], B. Di Girolamo[30], A. Di Mattia[153], B. Di Micco[135a,135b], R. Di Nardo[47], A. Di Simone[48], R. Di Sipio[20a,20b], D. Di Valentino[29], M. A. Diaz[32a], E. B. Diehl[88], J. Dietrich[42], T. A. Dietzsch[58a], S. Diglio[87], A. Dimitrievska[13a], J. Dingfelder[21], C. Dionisi[133a,133b], P. Dita[26a], S. Dita[26a], F. Dittus[30], F. Djama[84], T. Djobava[51b], M. A. B. do Vale[24c], A. Do Valle Wemans[125a,125g], T. K. O. Doan[5], D. Dobos[30], E. Dobson[77], C. Doglioni[49], T. Doherty[53], T. Dohmae[156], J. Dolejsi[128], Z. Dolezal[128], B. A. Dolgoshein[97,*], M. Donadelli[24d], S. Donati[123a,123b], P. Dondero[120a,120b], J. Donini[34], J. Dopke[30], A. Doria[103a], M. T. Dova[70], A. T. Doyle[53], M. Dris[10], J. Dubbert[88], S. Dube[15], E. Dubreuil[34], E. Duchovni[173], G. Duckeck[99], O. A. Ducu[26a], D. Duda[176], A. Dudarev[30], F. Dudziak[63],

L. Duflot[116], L. Duguid[76], M. Dührssen[30], M. Dunford[58a], H. Duran Yildiz[4a], M. Düren[52], A. Durglishvili[51b], M. Dwuznik[38a], M. Dyndal[38a], J. Ebke[99], W. Edson[2], N. C. Edwards[46], W. Ehrenfeld[21], T. Eifert[144], G. Eigen[14], K. Einsweiler[15], T. Ekelof[167], M. El Kacimi[136c], M. Ellert[167], S. Elles[5], F. Ellinghaus[82], N. Ellis[30], J. Elmsheuser[99], M. Elsing[30], D. Emeliyanov[130], Y. Enari[156], O. C. Endner[82], M. Endo[117], R. Engelmann[149], J. Erdmann[177], A. Ereditato[17], D. Eriksson[147a], G. Ernis[176], J. Ernst[2], M. Ernst[25], J. Ernwein[137], D. Errede[166], S. Errede[166], E. Ertel[82], M. Escalier[116], H. Esch[43], C. Escobar[124], B. Esposito[47], A. I. Etienvre[137], E. Etzion[154], H. Evans[60], L. Fabbri[20a,20b], G. Facini[30], R. M. Fakhrutdinov[129], S. Falciano[133a], J. Faltova[128], Y. Fang[33a], M. Fanti[90a,90b], A. Farbin[8], A. Farilla[135a], T. Farooque[12], S. Farrell[164], S. M. Farrington[171], P. Farthouat[30], F. Fassi[168], P. Fassnacht[30], D. Fassouliotis[9], A. Favareto[50a,50b], L. Fayard[116], P. Federic[145a], O. L. Fedin[122,j], W. Fedorko[169], M. Fehling-Kaschek[48], S. Feigl[30], L. Feligioni[84], C. Feng[33d], E. J. Feng[6], H. Feng[88], A. B. Fenyuk[129], S. Fernandez Perez[30], W. Fernando[6], S. Ferrag[53], J. Ferrando[53], V. Ferrara[42], A. Ferrari[167], P. Ferrari[106], R. Ferrari[120a], D. E. Ferreira de Lima[53], A. Ferrer[168], D. Ferrere[49], C. Ferretti[88], A. Ferretto Parodi[50a,50b], M. Fiascaris[31], F. Fiedler[82], A. Filipčič[74], M. Filipuzzi[42], F. Filthaut[105], M. Fincke-Keeler[170], K. D. Finelli[151], M. C. N. Fiolhais[125a,125c], L. Fiorini[168], A. Firan[40], J. Fischer[176], M. J. Fisher[110], W. C. Fisher[89], E. A. Fitzgerald[23], M. Flechl[48], I. Fleck[142], P. Fleischmann[175], S. Fleischmann[176], G. T. Fletcher[140], G. Fletcher[75], T. Flick[176], A. Floderus[80], L. R. Flores Castillo[174,k], A. C. Florez Bustos[160b], M. J. Flowerdew[100], A. Formica[137], A. Forti[83], D. Fortin[160a], D. Fournier[116], H. Fox[71], S. Fracchia[12], P. Francavilla[12], M. Franchini[20a,20b], S. Franchino[30], D. Francis[30], M. Franklin[57], S. Franz[61], M. Fraternali[120a,120b], S. T. French[28], C. Friedrich[42], F. Friedrich[44], D. Froidevaux[30], J. A. Frost[28], C. Fukunaga[157], E. Fullana Torregrosa[82], B. G. Fulsom[144], J. Fuster[168], C. Gabaldon[55], O. Gabizon[173], A. Gabrielli[20a,20b], A. Gabrielli[133a,133b], S. Gadatsch[106], S. Gadomski[49], G. Gagliardi[50a,50b], P. Gagnon[60], C. Galea[105], B. Galhardo[125a,125c], E. J. Gallas[119], V. Gallo[17], B. J. Gallop[130], P. Gallus[127], G. Galster[36], K. K. Gan[110], R. P. Gandrajula[62], J. Gao[33b,g], Y. S. Gao[144,e], F. M. Garay Walls[46], F. Garberson[177], C. García[168], J. E. García Navarro[168], M. Garcia-Sciveres[15], R. W. Gardner[31], N. Garelli[144], V. Garonne[30], C. Gatti[47], G. Gaudio[120a], B. Gaur[142], L. Gauthier[94], P. Gauzzi[133a,133b], I. L. Gavrilenko[95], C. Gay[169], G. Gaycken[21], E. N. Gazis[10], P. Ge[33d], Z. Gecse[169], C. N. P. Gee[130], D. A. A. Geerts[106], Ch. Geich-Gimbel[21], K. Gellerstedt[147a,147b], C. Gemme[50a], A. Gemmell[53], M. H. Genest[55], S. Gentile[133a,133b], M. George[54], S. George[76], D. Gerbaudo[164], A. Gershon[154], H. Ghazlane[136b], N. Ghodbane[34], B. Giacobbe[20a], S. Giagu[133a,133b], V. Giangiobbe[12], P. Giannetti[123a,123b], F. Gianotti[30], B. Gibbard[25], S. M. Gibson[76], M. Gilchriese[15], T. P. S. Gillam[28], D. Gillberg[30], D. M. Gingrich[3,d], N. Giokaris[9], M. P. Giordani[165a,165c], R. Giordano[103a,103b], F. M. Giorgi[16], P. F. Giraud[137], D. Giugni[90a], C. Giuliani[48], M. Giulini[58b], B. K. Gjelsten[118], I. Gkialas[155,l], L. K. Gladilin[98], C. Glasman[81], J. Glatzer[30], P. C. F. Glaysher[46], A. Glazov[42], G. L. Glonti[64], M. Goblirsch-Kolb[100], J. R. Goddard[75], J. Godfrey[143], J. Godlewski[30], C. Goeringer[82], S. Goldfarb[88], T. Golling[177], D. Golubkov[129], A. Gomes[125a,125b,125d], L. S. Gomez Fajardo[42], R. Gonçalo[125a], J. Goncalves Pinto Firmino Da Costa[42], L. Gonella[21], S. González de la Hoz[168], G. Gonzalez Parra[12], M. L. Gonzalez Silva[27], S. Gonzalez-Sevilla[49], L. Goossens[30], P. A. Gorbounov[96], H. A. Gordon[25], I. Gorelov[104], B. Gorini[30], E. Gorini[72a,72b], A. Gorišek[74], E. Gornicki[39], A. T. Goshaw[6], C. Gössling[43], M. I. Gostkin[64], M. Gouighri[136a], D. Goujdami[136c], M. P. Goulette[49], A. G. Goussiou[139], C. Goy[5], S. Gozpinar[23], H. M. X. Grabas[137], L. Graber[54], I. Grabowska-Bold[38a], P. Grafström[20a,20b], K-J. Grahn[42], J. Gramling[49], E. Gramstad[118], F. Grancagnolo[72a], S. Grancagnolo[16], V. Grassi[149], V. Gratchev[122], H. M. Gray[30], E. Graziani[135a], O. G. Grebenyuk[122], Z. D. Greenwood[78,m], K. Gregersen[36], I. M. Gregor[42], P. Grenier[144], J. Griffiths[8], A. A. Grillo[138], K. Grimm[71], S. Grinstein[12,n], Ph. Gris[34], Y. V. Grishkevich[98], J.-F. Grivaz[116], J. P. Grohs[44], A. Grohsjean[42], E. Gross[173], J. Grosse-Knetter[54], G. C. Grossi[134a,134b], J. Groth-Jensen[173], Z. J. Grout[150], K. Grybel[142], L. Guan[33b], F. Guescini[49], D. Guest[177], O. Gueta[154], C. Guicheney[34], E. Guido[50a,50b], T. Guillemin[116], S. Guindon[2], U. Gul[53], C. Gumpert[44], J. Gunther[127], J. Guo[35], S. Gupta[119], P. Gutierrez[112], N. G. Gutierrez Ortiz[53], C. Gutschow[77], N. Guttman[154], C. Guyot[137], C. Gwenlan[119], C. B. Gwilliam[73], A. Haas[109], C. Haber[15], H. K. Hadavand[8], N. Haddad[136e], P. Haefner[21], S. Hageböck[21], Z. Hajduk[39], H. Hakobyan[178], M. Haleem[42], D. Hall[119], G. Halladjian[89], K. Hamacher[176], P. Hamal[114], K. Hamano[87], M. Hamer[54], A. Hamilton[146a], S. Hamilton[162], P. G. Hamnett[42], L. Han[33b], K. Hanagaki[117], K. Hanawa[156], M. Hance[15], P. Hanke[58a], J. B. Hansen[36], J. D. Hansen[36], P. H. Hansen[36], K. Hara[161], A. S. Hard[174], T. Harenberg[176], S. Harkusha[91], D. Harper[88], R. D. Harrington[46], O. M. Harris[139], P. F. Harrison[171], F. Hartjes[106], A. Harvey[56], S. Hasegawa[102], Y. Hasegawa[141], A. Hasib[112], S. Hassani[137], S. Haug[17], M. Hauschild[30], R. Hauser[89], M. Havranek[126], C. M. Hawkes[18], R. J. Hawkings[30], A. D. Hawkins[80], T. Hayashi[161], D. Hayden[89], C. P. Hays[119], H. S. Hayward[73], S. J. Haywood[130], S. J. Head[18], T. Heck[82], V. Hedberg[80], L. Heelan[8], S. Heim[121], T. Heim[176], B. Heinemann[15], L. Heinrich[109], S. Heisterkamp[36], J. Hejbal[126], L. Helary[22], C. Heller[99], M. Heller[30], S. Hellman[147a,147b], D. Hellmich[21], C. Helsens[30], J. Henderson[119], R. C. W. Henderson[71], C. Hengler[42], A. Henrichs[177], A. M. Henriques Correia[30], S. Henrot-Versille[116], C. Hensel[54], G. H. Herbert[16], Y. Hernández Jiménez[168], R. Herrberg-Schubert[16], G. Herten[48], R. Hertenberger[99], L. Hervas[30], G. G. Hesketh[77], N. P. Hessey[106], R. Hickling[75], E. Higón-Rodriguez[168], J. C. Hill[28], K. H. Hiller[42], S. Hillert[21], S. J. Hillier[18], I. Hinchliffe[15], E. Hines[121], M. Hirose[117], D. Hirschbuehl[176], J. Hobbs[149], N. Hod[106], M. C. Hodgkinson[140], P. Hodgson[140], A. Hoecker[30], M. R. Hoeferkamp[104], J. Hoffman[40], D. Hoffmann[84], J. I. Hofmann[58a], M. Hohlfeld[82], T. R.

Holmes[15], T. M. Hong[121], L. Hooft van Huysduynen[109], J-Y. Hostachy[55], S. Hou[152], A. Hoummada[136a], J. Howard[119], J. Howarth[42], M. Hrabovsky[114], I. Hristova[16], J. Hrivnac[116], T. Hryn'ova[5], P. J. Hsu[82], S.-C. Hsu[139], D. Hu[35], X. Hu[25], Y. Huang[42], Z. Hubacek[30], F. Hubaut[84], F. Huegging[21], T. B. Huffman[119], E. W. Hughes[35], G. Hughes[71], M. Huhtinen[30], T. A. Hülsing[82], M. Hurwitz[15], N. Huseynov[64,b], J. Huston[89], J. Huth[57], G. Iacobucci[49], G. Iakovidis[10], I. Ibragimov[142], L. Iconomidou-Fayard[116], E. Ideal[177], P. Iengo[103a], O. Igonkina[106], T. Iizawa[172], Y. Ikegami[65], K. Ikematsu[142], M. Ikeno[65], D. Iliadis[155], N. Ilic[159], Y. Inamaru[66], T. Ince[100], P. Ioannou[9], M. Iodice[135a], K. Iordanidou[9], V. Ippolito[57], A. Irles Quiles[168], C. Isaksson[167], M. Ishino[67], M. Ishitsuka[158], R. Ishmukhametov[110], C. Issever[119], S. Istin[19a], J. M. Iturbe Ponce[83], A. V. Ivashin[129], W. Iwanski[39], H. Iwasaki[65], J. M. Izen[41], V. Izzo[103a], B. Jackson[121], J. N. Jackson[73], M. Jackson[73], P. Jackson[1], M. R. Jaekel[30], V. Jain[2], K. Jakobs[48], S. Jakobsen[36], T. Jakoubek[126], J. Jakubek[127], D. O. Jamin[152], D. K. Jana[78], E. Jansen[77], H. Jansen[30], J. Janssen[21], M. Janus[171], G. Jarlskog[80], T. Javůrek[48], L. Jeanty[15], G.-Y. Jeng[151], D. Jennens[87], P. Jenni[48,o], J. Jentzsch[43], C. Jeske[171], S. Jézéquel[5], H. Ji[174], W. Ji[82], J. Jia[149], Y. Jiang[33b], M. Jimenez Belenguer[42], S. Jin[33a], A. Jinaru[26a], O. Jinnouchi[158], M. D. Joergensen[36], K. E. Johansson[147a], P. Johansson[140], K. A. Johns[7], K. Jon-And[147a,147b], G. Jones[171], R. W. L. Jones[71], T. J. Jones[73], J. Jongmanns[58a], P. M. Jorge[125a,125b], K. D. Joshi[83], J. Jovicevic[148], X. Ju[174], C. A. Jung[43], R. M. Jungst[30], P. Jussel[61], A. Juste Rozas[12,n], M. Kaci[168], A. Kaczmarska[39], M. Kado[116], H. Kagan[110], M. Kagan[144], E. Kajomovitz[45], S. Kama[40], N. Kanaya[156], M. Kaneda[30], S. Kaneti[28], T. Kanno[158], V. A. Kantserov[97], J. Kanzaki[65], B. Kaplan[109], A. Kapliy[31], D. Kar[53], K. Karakostas[10], N. Karastathis[10], M. Karnevskiy[82], S. N. Karpov[64], K. Karthik[109], V. Kartvelishvili[71], A. N. Karyukhin[129], L. Kashif[174], G. Kasieczka[58b], R. D. Kass[110], A. Kastanas[14], Y. Kataoka[156], A. Katre[49], J. Katzy[42], V. Kaushik[7], K. Kawagoe[69], T. Kawamoto[156], G. Kawamura[54], S. Kazama[156], V. F. Kazanin[108], M. Y. Kazarinov[64], R. Keeler[170], R. Kehoe[40], M. Keil[54], J. S. Keller[42], H. Keoshkerian[5], O. Kepka[126], B. P. Kerševan[74], S. Kersten[176], K. Kessoku[156], J. Keung[159], F. Khalil-zada[11], H. Khandanyan[147a,147b], A. Khanov[113], A. Khodinov[97], A. Khomich[58a], T. J. Khoo[28], G. Khoriauli[21], A. Khoroshilov[176], V. Khovanskiy[96], E. Khramov[64], J. Khubua[51b], H. Y. Kim[8], H. Kim[147a,147b], S. H. Kim[161], N. Kimura[172], O. Kind[16], B. T. King[73], M. King[168], R. S. B. King[119], S. B. King[169], J. Kirk[130], A. E. Kiryunin[100], T. Kishimoto[66], D. Kisielewska[38a], F. Kiss[48], T. Kitamura[66], T. Kittelmann[124], K. Kiuchi[161], E. Kladiva[145b], M. Klein[73], U. Klein[73], K. Kleinknecht[82], P. Klimek[147a,147b], A. Klimentov[25], R. Klingenberg[43], J. A. Klinger[83], E. B. Klinkby[36], T. Klioutchnikova[30], P. F. Klok[105], E.-E. Kluge[58a], P. Kluit[106], S. Kluth[100], E. Kneringer[61], E. B. F. G. Knoops[84], A. Knue[53], T. Kobayashi[156], M. Kobel[44], M. Kocian[144], P. Kodys[128], P. Koevesarki[21], T. Koffas[29], E. Koffeman[106], L. A. Kogan[119], S. Kohlmann[176], Z. Kohout[127], T. Kohriki[65], T. Koi[144], H. Kolanoski[16], I. Koletsou[5], J. Koll[89], A. A. Komar[95,*], Y. Komori[156], T. Kondo[65], K. Köneke[48], A. C. König[105], S. König[82], T. Kono[65,p], R. Konoplich[109,q], N. Konstantinidis[77], R. Kopeliansky[153], S. Koperny[38a], L. Köpke[82], A. K. Kopp[48], K. Korcyl[39], K. Kordas[155], A. Korn[77], A. A. Korol[108,r], I. Korolkov[12], E. V. Korolkova[140], V. A. Korotkov[129], O. Kortner[100], S. Kortner[100], V. V. Kostyukhin[21], V. M. Kotov[64], A. Kotwal[45], C. Kourkoumelis[9], V. Kouskoura[155], A. Koutsman[160a], R. Kowalewski[170], T. Z. Kowalski[38a], W. Kozanecki[137], A. S. Kozhin[129], V. Kral[127], V. A. Kramarenko[98], G. Kramberger[74], D. Krasnopevtsev[97], M. W. Krasny[79], A. Krasznahorkay[30], J. K. Kraus[21], A. Kravchenko[25], S. Kreiss[109], M. Kretz[58c], J. Kretzschmar[73], K. Kreutzfeldt[52], P. Krieger[159], K. Kroeninger[54], H. Kroha[100], J. Kroll[121], J. Kroseberg[21], J. Krstic[13a], U. Kruchonak[64], H. Krüger[21], T. Kruker[17], N. Krumnack[63], Z. V. Krumshteyn[64], A. Kruse[174], M. C. Kruse[45], M. Kruskal[22], T. Kubota[87], S. Kuday[4a], S. Kuehn[48], A. Kugel[58c], A. Kuhl[138], T. Kuhl[42], V. Kukhtin[64], Y. Kulchitsky[91], S. Kuleshov[32b], M. Kuna[133a,133b], J. Kunkle[121], A. Kupco[126], H. Kurashige[66], Y. A. Kurochkin[91], R. Kurumida[66], V. Kus[126], E. S. Kuwertz[148], M. Kuze[158], J. Kvita[143], A. La Rosa[49], L. La Rotonda[37a,37b], L. Labarga[81], C. Lacasta[168], F. Lacava[133a,133b], J. Lacey[29], H. Lacker[16], D. Lacour[79], V. R. Lacuesta[168], E. Ladygin[64], R. Lafaye[5], B. Laforge[79], T. Lagouri[177], S. Lai[48], H. Laier[58a], L. Lambourne[77], S. Lammers[60], C. L. Lampen[7], W. Lampl[7], E. Lançon[137], U. Landgraf[48], M. P. J. Landon[75], V. S. Lang[58a], C. Lange[42], A. J. Lankford[164], F. Lanni[25], K. Lantzsch[30], S. Laplace[79], C. Lapoire[21], J. F. Laporte[137], T. Lari[90a], M. Lassnig[30], P. Laurelli[47], V. Lavorini[37a,37b], W. Lavrijsen[15], A. T. Law[138], P. Laycock[73], B. T. Le[55], O. Le Dortz[79], E. Le Guirriec[84], E. Le Menedeu[12], T. LeCompte[6], F. Ledroit-Guillon[55], C. A. Lee[152], H. Lee[106], J. S. H. Lee[117], S. C. Lee[152], L. Lee[177], G. Lefebvre[79], M. Lefebvre[170], F. Legger[99], C. Leggett[15], A. Lehan[73], M. Lehmacher[21], G. Lehmann Miotto[30], X. Lei[7], A. G. Leister[177], M. A. L. Leite[24d], R. Leitner[128], D. Lellouch[173], B. Lemmer[54], K. J. C. Leney[77], T. Lenz[106], G. Lenzen[176], B. Lenzi[30], R. Leone[7], K. Leonhardt[44], S. Leontsinis[10], C. Leroy[94], C. G. Lester[28], C. M. Lester[121], J. Levêque[5], D. Levin[88], L. J. Levinson[173], M. Levy[18], A. Lewis[119], G. H. Lewis[109], A. M. Leyko[21], M. Leyton[41], B. Li[33b,s], B. Li[84], H. Li[149], H. L. Li[31], S. Li[45], X. Li[88], Y. Li[33c,t], Z. Liang[119,u], H. Liao[34], B. Liberti[134a], P. Lichard[30], K. Lie[166], J. Liebal[21], W. Liebig[14], C. Limbach[21], A. Limosani[87], M. Limper[62], S. C. Lin[152,v], F. Linde[106], B. E. Lindquist[149], J. T. Linnemann[89], E. Lipeles[121], A. Lipniacka[14], M. Lisovyi[42], T. M. Liss[166], D. Lissauer[25], A. Lister[169], A. M. Litke[138], B. Liu[152], D. Liu[152], J. B. Liu[33b], K. Liu[33b,w], L. Liu[88], M. Liu[45], M. Liu[33b], Y. Liu[33b], M. Livan[120a,120b], S. S. A. Livermore[119], A. Lleres[55], J. Llorente Merino[81], S. L. Lloyd[75], F. Lo Sterzo[152], E. Lobodzinska[42], P. Loch[7], W. S. Lockman[138], T. Loddenkoetter[21], F. K. Loebinger[83], A. E. Loevschall-Jensen[36], A. Loginov[177], C. W. Loh[169], T. Lohse[16], K. Lohwasser[48], M. Lokajicek[126], V. P. Lombardo[5], J. D. Long[88], R. E. Long[71], L. Lopes[125a], D. Lopez Mateos[57],

B. Lopez Paredes[140], J. Lorenz[99], N. Lorenzo Martinez[60], M. Losada[163], P. Loscutoff[15], M. J. Losty[160a,*], X. Lou[41], A. Lounis[116], J. Love[6], P. A. Love[71], A. J. Lowe[144,e], F. Lu[33a], H. J. Lubatti[139], C. Luci[133a,133b], A. Lucotte[55], F. Luehring[60], W. Lukas[61], L. Luminari[133a], O. Lundberg[147a,147b], B. Lund-Jensen[148], M. Lungwitz[82], D. Lynn[25], R. Lysak[126], E. Lytken[80], H. Ma[25], L. L. Ma[33d], G. Maccarrone[47], A. Macchiolo[100], B. Maček[74], J. Machado Miguens[125a,125b], D. Macina[30], D. Madaffari[84], R. Madar[48], H. J. Maddocks[71], W. F. Mader[44], A. Madsen[167], M. Maeno[8], T. Maeno[25], E. Magradze[54], K. Mahboubi[48], J. Mahlstedt[106], S. Mahmoud[73], C. Maiani[137], C. Maidantchik[24a], A. Maio[125a,125b,125d], S. Majewski[115], Y. Makida[65], N. Makovec[116], P. Mal[137,x], B. Malaescu[79], Pa. Malecki[39], V. P. Maleev[122], F. Malek[55], U. Mallik[62], D. Malon[6], C. Malone[144], S. Maltezos[10], V. M. Malyshev[108], S. Malyukov[30], J. Mamuzic[13b], B. Mandelli[30], L. Mandelli[90a], I. Mandić[74], R. Mandrysch[62], J. Maneira[125a,125b], A. Manfredini[100], L. Manhaes de Andrade Filho[24b], J. A. Manjarres Ramos[160b], A. Mann[99], P. M. Manning[138], A. Manousakis-Katsikakis[9], B. Mansoulie[137], R. Mantifel[86], L. Mapelli[30], L. March[168], J. F. Marchand[29], F. Marchese[134a,134b], G. Marchiori[79], M. Marcisovsky[126], C. P. Marino[170], C. N. Marques[125a], F. Marroquim[24a], S. P. Marsden[83], Z. Marshall[15], L. F. Marti[17], S. Marti-Garcia[168], B. Martin[30], B. Martin[89], T. A. Martin[171], V. J. Martin[46], B. Martin dit Latour[14], H. Martinez[137], M. Martinez[12,n], S. Martin-Haugh[130], A. C. Martyniuk[77], M. Marx[139], F. Marzano[133a], A. Marzin[30], L. Masetti[82], T. Mashimo[156], R. Mashinistov[95], J. Masik[83], A. L. Maslennikov[108], I. Massa[20a,20b], N. Massol[5], P. Mastrandrea[149], A. Mastroberardino[37a,37b], T. Masubuchi[156], H. Matsunaga[156], T. Matsushita[66], P. Mättig[176], S. Mättig[42], J. Mattmann[82], J. Maurer[26a], S. J. Maxfield[73], D. A. Maximov[108,r], R. Mazini[152], L. Mazzaferro[134a,134b], G. Mc Goldrick[159], S. P. Mc Kee[88], A. McCarn[88], R. L. McCarthy[149], T. G. McCarthy[29], N. A. McCubbin[130], K. W. McFarlane[56,*], J. A. Mcfayden[77], G. Mchedlidze[54], T. Mclaughlan[18], S. J. McMahon[130], R. A. McPherson[170,i], A. Meade[85], J. Mechnich[106], M. Medinnis[42], S. Meehan[31], R. Meera-Lebbai[112], S. Mehlhase[36], A. Mehta[73], K. Meier[58a], C. Meineck[99], B. Meirose[80], C. Melachrinos[31], B. R. Mellado Garcia[146c], F. Meloni[90a,90b], L. Mendoza Navas[163], A. Mengarelli[20a,20b], S. Menke[100], E. Meoni[162], K. M. Mercurio[57], S. Mergelmeyer[21], N. Meric[137], P. Mermod[49], L. Merola[103a,103b], C. Meroni[90a], F. S. Merritt[31], H. Merritt[110], A. Messina[30,y], J. Metcalfe[25], A. S. Mete[164], C. Meyer[82], C. Meyer[31], J-P. Meyer[137], J. Meyer[30], R. P. Middleton[130], S. Migas[73], L. Mijović[137], G. Mikenberg[173], M. Mikestikova[126], M. Mikuž[74], D. W. Miller[31], C. Mills[46], A. Milov[173], D. A. Milstead[147a,147b], D. Milstein[173], A. A. Minaenko[129], M. Miñano Moya[168], I. A. Minashvili[64], A. I. Mincer[109], B. Mindur[38a], M. Mineev[64], Y. Ming[174], L. M. Mir[12], G. Mirabelli[133a], T. Mitani[172], J. Mitrevski[99], V. A. Mitsou[168], S. Mitsui[65], A. Miucci[49], P. S. Miyagawa[140], J. U. Mjörnmark[80], T. Moa[147a,147b], K. Mochizuki[84], V. Moeller[28], S. Mohapatra[35], W. Mohr[48], S. Molander[147a,147b], R. Moles-Valls[168], K. Mönig[42], C. Monini[55], J. Monk[36], E. Monnier[84], J. Montejo Berlingen[12], F. Monticelli[70], S. Monzani[133a,133b], R. W. Moore[3], C. Mora Herrera[49], A. Moraes[53], N. Morange[62], J. Morel[54], D. Moreno[82], M. Moreno Llácer[54], P. Morettini[50a], M. Morgenstern[44], M. Morii[57], S. Moritz[82], A. K. Morley[148], G. Mornacchi[30], J. D. Morris[75], L. Morvaj[102], H. G. Moser[100], M. Mosidze[51b], J. Moss[110], R. Mount[144], E. Mountricha[25], S. V. Mouraviev[95,*], E. J. W. Moyse[85], S. Muanza[84], R. D. Mudd[18], F. Mueller[58a], J. Mueller[124], K. Mueller[21], T. Mueller[28], T. Mueller[82], D. Muenstermann[49], Y. Munwes[154], J. A. Murillo Quijada[18], W. J. Murray[130,171], E. Musto[153], A. G. Myagkov[129,z], M. Myska[126], O. Nackenhorst[54], J. Nadal[54], K. Nagai[61], R. Nagai[158], Y. Nagai[84], K. Nagano[65], A. Nagarkar[110], Y. Nagasaka[59], M. Nagel[100], A. M. Nairz[30], Y. Nakahama[30], K. Nakamura[65], T. Nakamura[156], I. Nakano[111], H. Namasivayam[41], G. Nanava[21], R. Narayan[58b], T. Nattermann[21], T. Naumann[42], G. Navarro[163], R. Nayyar[7], H. A. Neal[88], P. Yu. Nechaeva[95], T. J. Neep[83], A. Negri[120a,120b], G. Negri[30], M. Negrini[20a], S. Nektarijevic[49], A. Nelson[164], T. K. Nelson[144], S. Nemecek[126], P. Nemethy[109], A. A. Nepomuceno[24a], M. Nessi[30,aa], M. S. Neubauer[166], M. Neumann[176], R. M. Neves[109], P. Nevski[25], P. R. Newman[18], D. H. Nguyen[6], R. B. Nickerson[119], R. Nicolaidou[137], B. Nicquevert[30], J. Nielsen[138], N. Nikiforou[35], A. Nikiforov[16], V. Nikolaenko[129,z], I. Nikolic-Audit[79], K. Nikolics[49], K. Nikolopoulos[18], P. Nilsson[8], Y. Ninomiya[156], A. Nisati[133a], R. Nisius[100], T. Nobe[158], L. Nodulman[6], M. Nomachi[117], I. Nomidis[155], S. Norberg[112], M. Nordberg[30], S. Nowak[100], M. Nozaki[65], L. Nozka[114], K. Ntekas[10], G. Nunes Hanninger[87], T. Nunnemann[99], E. Nurse[77], F. Nuti[87], B. J. O'Brien[46], F. O'Grady[7], D. C. O'Neil[143], V. O'Shea[53], F. G. Oakham[29,d], H. Oberlack[100], T. Obermann[21], J. Ocariz[79], A. Ochi[66], M. I. Ochoa[77], S. Oda[69], S. Odaka[65], H. Ogren[60], A. Oh[83], S. H. Oh[45], C. C. Ohm[30], H. Ohman[167], T. Ohshima[102], W. Okamura[117], H. Okawa[25], Y. Okumura[31], T. Okuyama[156], A. Olariu[26a], A. G. Olchevski[64], S. A. Olivares Pino[46], D. Oliveira Damazio[25], E. Oliver Garcia[168], D. Olivito[121], A. Olszewski[39], J. Olszowska[39], A. Onofre[125a,125e], P. U. E. Onyisi[31,ab], C. J. Oram[160a], M. J. Oreglia[31], Y. Oren[154], D. Orestano[135a,135b], N. Orlando[72a,72b], C. Oropeza Barrera[53], R. S. Orr[159], B. Osculati[50a,50b], R. Ospanov[121], G. Otero y Garzon[27], H. Otono[69], M. Ouchrif[136d], E. A. Ouellette[170], F. Ould-Saada[118], A. Ouraou[137], K. P. Oussoren[106], Q. Ouyang[33a], A. Ovcharova[15], M. Owen[83], V. E. Ozcan[19a], N. Ozturk[8], K. Pachal[119], A. Pacheco Pages[12], C. Padilla Aranda[12], M. Pagáčová[48], S. Pagan Griso[15], E. Paganis[140], C. Pahl[100], F. Paige[25], P. Pais[85], K. Pajchel[118], G. Palacino[160b], S. Palestini[30], D. Pallin[34], A. Palma[125a,125b], J. D. Palmer[18], Y. B. Pan[174], E. Panagiotopoulou[10], J. G. Panduro Vazquez[76], P. Pani[106], N. Panikashvili[88], S. Panitkin[25], D. Pantea[26a], L. Paolozzi[134a,134b], Th. D. Papadopoulou[10], K. Papageorgiou[155,l], A. Paramonov[6], D. Paredes Hernandez[34], M. A. Parker[28], F. Parodi[50a,50b], J. A. Parsons[35], U. Parzefall[48], E. Pasqualucci[133a], S. Passaggio[50a], A. Passeri[135a], F. Pastore[135a,135b,*], Fr. Pastore[76], G. Pásztor[49,ac], S. Pataraia[176], N. D.

Patel[151], J. R. Pater[83], S. Patricelli[103a,103b], T. Pauly[30], J. Pearce[170], M. Pedersen[118], S. Pedraza Lopez[168], R. Pedro[125a,125b], S. V. Peleganchuk[108], D. Pelikan[167], H. Peng[33b], B. Penning[31], J. Penwell[60], D. V. Perepelitsa[25], E. Perez Codina[160a], M. T. Pérez García-Estañ[168], V. Perez Reale[35], L. Perini[90a,90b], H. Pernegger[30], R. Perrino[72a], R. Peschke[42], V. D. Peshekhonov[64], K. Peters[30], R. F. Y. Peters[83], B. A. Petersen[87], J. Petersen[30], T. C. Petersen[36], E. Petit[42], A. Petridis[147a,147b], C. Petridou[155], E. Petrolo[133a], F. Petrucci[135a,135b], M. Petteni[143], N. E. Pettersson[158], R. Pezoa[32b], P. W. Phillips[130], G. Piacquadio[144], E. Pianori[171], A. Picazio[49], E. Piccaro[75], M. Piccinini[20a,20b], S. M. Piec[42], R. Piegaia[27], D. T. Pignotti[110], J. E. Pilcher[31], A. D. Pilkington[77], J. Pina[125a,125b,125d], M. Pinamonti[165a,165c,ad], A. Pinder[119], J. L. Pinfold[3], A. Pingel[36], B. Pinto[125a], S. Pires[79], C. Pizio[90a,90b], M.-A. Pleier[25], V. Pleskot[128], E. Plotnikova[64], P. Plucinski[147a,147b], S. Poddar[58a], F. Podlyski[34], R. Poettgen[82], L. Poggioli[116], D. Pohl[21], M. Pohl[49], G. Polesello[120a], A. Policicchio[37a,37b], R. Polifka[159], A. Polini[20a], C. S. Pollard[45], V. Polychronakos[25], K. Pommès[30], L. Pontecorvo[133a], B. G. Pope[89], G. A. Popeneciu[26b], D. S. Popovic[13a], A. Poppleton[30], X. Portell Bueso[12], G. E. Pospelov[100], S. Pospisil[127], K. Potamianos[15], I. N. Potrap[64], C. J. Potter[150], C. T. Potter[115], G. Poulard[30], J. Poveda[60], V. Pozdnyakov[64], R. Prabhu[77], P. Pralavorio[84], A. Pranko[15], S. Prasad[30], R. Pravahan[8], S. Prell[63], D. Price[83], J. Price[73], L. E. Price[6], D. Prieur[124], M. Primavera[72a], M. Proissl[46], K. Prokofiev[47], F. Prokoshin[32b], E. Protopapadaki[137], S. Protopopescu[25], J. Proudfoot[6], M. Przybycien[38a], H. Przysiezniak[5], E. Ptacek[115], E. Pueschel[85], D. Puldon[149], M. Purohit[25,ae], P. Puzo[116], Y. Pylypchenko[62], J. Qian[88], G. Qin[53], A. Quadt[54], D. R. Quarrie[15], W. B. Quayle[165a,165b], D. Quilty[53], A. Qureshi[160b], V. Radeka[25], V. Radescu[42], S. K. Radhakrishnan[149], P. Radloff[115], P. Rados[87], F. Ragusa[90a,90b], G. Rahal[179], S. Rajagopalan[25], M. Rammensee[30], M. Rammes[142], A. S. Randle-Conde[40], C. Rangel-Smith[79], K. Rao[164], F. Rauscher[99], T. C. Rave[48], T. Ravenscroft[53], M. Raymond[30], A. L. Read[118], D. M. Rebuzzi[120a,120b], A. Redelbach[175], G. Redlinger[25], R. Reece[138], K. Reeves[41], L. Rehnisch[16], A. Reinsch[115], H. Reisin[27], M. Relich[164], C. Rembser[30], Z. L. Ren[152], A. Renaud[116], M. Rescigno[133a], S. Resconi[90a], O. L. Rezanova[108,r], P. Reznicek[128], R. Rezvani[94], R. Richter[100], M. Ridel[79], P. Rieck[16], M. Rijssenbeek[149], A. Rimoldi[120a,120b], L. Rinaldi[20a], E. Ritsch[61], I. Riu[12], F. Rizatdinova[113], E. Rizvi[75], S. H. Robertson[86,i], A. Robichaud-Veronneau[119], D. Robinson[28], J. E. M. Robinson[83], A. Robson[53], C. Roda[123a,123b], L. Rodrigues[30], S. Roe[30], O. Røhne[118], S. Rolli[162], A. Romaniouk[97], M. Romano[20a,20b], G. Romeo[27], E. Romero Adam[168], N. Rompotis[139], L. Roos[79], E. Ros[168], S. Rosati[133a], K. Rosbach[49], A. Rose[150], M. Rose[76], P. L. Rosendahl[14], O. Rosenthal[142], V. Rossetti[147a,147b], E. Rossi[103a,103b], L. P. Rossi[50a], R. Rosten[139], M. Rotaru[26a], I. Roth[173], J. Rothberg[139], D. Rousseau[116], C. R. Royon[137], A. Rozanov[84], Y. Rozen[153], X. Ruan[146c], F. Rubbo[12], I. Rubinskiy[42], V. I. Rud[98], C. Rudolph[44], M. S. Rudolph[159], F. Rühr[48], A. Ruiz-Martinez[63], Z. Rurikova[48], N. A. Rusakovich[64], A. Ruschke[99], J. P. Rutherfoord[7], N. Ruthmann[48], Y. F. Ryabov[122], M. Rybar[128], G. Rybkin[116], N. C. Ryder[119], A. F. Saavedra[151], S. Sacerdoti[27], A. Saddique[3], I. Sadeh[154], H. F-W. Sadrozinski[138], R. Sadykov[64], F. Safai Tehrani[133a], H. Sakamoto[156], Y. Sakurai[172], G. Salamanna[75], A. Salamon[134a], M. Saleem[112], D. Salek[106], P. H. Sales De Bruin[139], D. Salihagic[100], A. Salnikov[144], J. Salt[168], B. M. Salvachua Ferrando[6], D. Salvatore[37a,37b], F. Salvatore[150], A. Salvucci[105], A. Salzburger[30], D. Sampsonidis[155], A. Sanchez[103a,103b], J. Sánchez[168], V. Sanchez Martinez[168], H. Sandaker[14], H. G. Sander[82], M. P. Sanders[99], M. Sandhoff[176], T. Sandoval[28], C. Sandoval[163], R. Sandstroem[100], D. P. C. Sankey[130], A. Sansoni[47], C. Santoni[34], R. Santonico[134a,134b], H. Santos[125a], I. Santoyo Castillo[150], K. Sapp[124], A. Sapronov[64], J. G. Saraiva[125a,125d], B. Sarrazin[21], G. Sartisohn[176], O. Sasaki[65], Y. Sasaki[156], G. Sauvage[5,*], E. Sauvan[5], P. Savard[159d], D. O. Savu[30], C. Sawyer[119], L. Sawyer[78,m], D. H. Saxon[53], J. Saxon[121], C. Sbarra[20a], A. Sbrizzi[3], T. Scanlon[30], D. A. Scannicchio[164], M. Scarcella[151], J. Schaarschmidt[173], P. Schacht[100], D. Schaefer[121], R. Schaefer[42], A. Schaelicke[46], S. Schaepe[21], S. Schaetzel[58b], U. Schäfer[82], A. C. Schaffer[116], D. Schaile[99], R. D. Schamberger[149], V. Scharf[58a], V. A. Schegelsky[122], D. Scheirich[128], M. Schernau[164], M. I. Scherzer[35], C. Schiavi[50a,50b], J. Schieck[99], C. Schillo[48], M. Schioppa[37a,37b], S. Schlenker[30], E. Schmidt[48], K. Schmieden[30], C. Schmitt[82], C. Schmitt[99], S. Schmitt[58b], B. Schneider[17], Y. J. Schnellbach[73], U. Schnoor[44], L. Schoeffel[137], A. Schoening[58b], B. D. Schoenrock[89], A. L. S. Schorlemmer[54], M. Schott[82], D. Schouten[160a], J. Schovancova[25], S. Schramm[159], M. Schreyer[175], C. Schroeder[82], N. Schuh[82], M. J. Schultens[21], H.-C. Schultz-Coulon[58a], H. Schulz[16], M. Schumacher[48], B. A. Schumm[138], Ph. Schune[137], A. Schwartzman[144], Ph. Schwegler[100], Ph. Schwemling[137], R. Schwienhorst[89], J. Schwindling[137], T. Schwindt[21], M. Schwoerer[5], F. G. Sciacca[17], E. Scifo[116], G. Sciolla[23], W. G. Scott[130], F. Scuri[123a,123b], F. Scutti[21], J. Searcy[88], G. Sedov[42], E. Sedykh[122], S. C. Seidel[104], A. Seiden[138], F. Seifert[127], J. M. Seixas[24a], G. Sekhniaidze[103a], S. J. Sekula[40], K. E. Selbach[46], D. M. Seliverstov[122,*], G. Sellers[73], N. Semprini-Cesari[20a,20b], C. Serfon[30], L. Serin[116], L. Serkin[54], T. Serre[84], R. Seuster[160a], H. Severini[112], F. Sforza[100], A. Sfyrla[30], E. Shabalina[54], M. Shamim[115], L. Y. Shan[33a], J. T. Shank[22], Q. T. Shao[87], M. Shapiro[15], P. B. Shatalov[96], K. Shaw[165a,165b], P. Sherwood[77], S. Shimizu[66], C. O. Shimmin[164], M. Shimojima[101], M. Shiyakova[64], A. Shmeleva[95], M. J. Shochet[31], D. Short[119], S. Shrestha[63], E. Shulga[97], M. A. Shupe[7], S. Shushkevich[42], P. Sicho[126], D. Sidorov[113], A. Sidoti[133a], F. Siegert[44], Dj. Sijacki[13a], O. Silbert[173], J. Silva[125a,125d], Y. Silver[154], D. Silverstein[144], S. B. Silverstein[147a], V. Simak[127], O. Simard[5], Lj. Simic[13a], S. Simion[116], E. Simioni[82], B. Simmons[77], R. Simoniello[90a,90b], M. Simonyan[36], P. Sinervo[159], N. B. Sinev[115], V. Sipica[142], G. Siragusa[175], A. Sircar[78], A. N. Sisakyan[64,*], S. Yu. Sivoklokov[98], J. Sjölin[147a,147b], T. B. Sjursen[14], L. A. Skinnari[15], H. P. Skottowe[57], K. Yu. Skovpen[108], P. Skubic[112], M. Slater[18], T. Slavicek[127], K. Sliwa[162], V. Smakhtin[173],

B. H. Smart[46], L. Smestad[118], S. Yu. Smirnov[97], Y. Smirnov[97], L. N. Smirnova[98,af], O. Smirnova[80], K. M. Smith[53], M. Smizanska[71], K. Smolek[127], A. A. Snesarev[95], G. Snidero[75], S. Snyder[25], R. Sobie[170,i], F. Socher[44], A. Soffer[154], D. A. Soh[152,u], C. A. Solans[30], M. Solar[127], J. Solc[127], E. Yu. Soldatov[97], U. Soldevila[168], E. Solfaroli Camillocci[133a,133b], A. A. Solodkov[129], O. V. Solovyanov[129], V. Solovyev[122], P. Sommer[48], H. Y. Song[33b], N. Soni[1], A. Sood[15], B. Sopko[127], V. Sopko[127], V. Sorin[12], M. Sosebee[8], R. Soualah[165a,165c], P. Soueid[94], A. M. Soukharev[108], D. South[42], S. Spagnolo[72a,72b], F. Spanò[76], W. R. Spearman[57], R. Spighi[20a], G. Spigo[30], M. Spousta[128], T. Spreitzer[159], B. Spurlock[8], R. D. St. Denis[53], S. Staerz[44], J. Stahlman[121], R. Stamen[58a], E. Stanecka[39], R. W. Stanek[6], C. Stanescu[135a], M. Stanescu-Bellu[42], M. M. Stanitzki[42], S. Stapnes[118], E. A. Starchenko[129], J. Stark[55], P. Staroba[126], P. Starovoitov[42], R. Staszewski[39], P. Stavina[145a,*], G. Steele[53], P. Steinberg[25], B. Stelzer[143], H. J. Stelzer[30], O. Stelzer-Chilton[160a], H. Stenzel[52], S. Stern[100], G. A. Stewart[53], J. A. Stillings[21], M. C. Stockton[86], M. Stoebe[86], K. Stoerig[48], G. Stoicea[26a], P. Stolte[54], S. Stonjek[100], A. R. Stradling[8], A. Straessner[44], J. Strandberg[148], S. Strandberg[147a,147b], A. Strandlie[118], E. Strauss[144], M. Strauss[112], P. Strizenec[145b], R. Ströhmer[175], D. M. Strom[115], R. Stroynowski[40], S. A. Stucci[17], B. Stugu[14], N. A. Styles[42], D. Su[144], J. Su[124], HS. Subramania[3], R. Subramaniam[78], A. Succurro[12], Y. Sugaya[117], C. Suhr[107], M. Suk[127], V. V. Sulin[95], S. Sultansoy[4c], T. Sumida[67], X. Sun[33a], J. E. Sundermann[48], K. Suruliz[140], G. Susinno[37a,37b], M. R. Sutton[150], Y. Suzuki[65], M. Svatos[126], S. Swedish[169], M. Swiatlowski[144], I. Sykora[145a], T. Sykora[128], D. Ta[89], K. Tackmann[42], J. Taenzer[159], A. Taffard[164], R. Tafirout[160a], N. Taiblum[154], Y. Takahashi[102], H. Takai[25], R. Takashima[68], H. Takeda[66], T. Takeshita[141], Y. Takubo[65], M. Talby[84], A. A. Talyshev[108,r], J. Y. C. Tam[175], M. C. Tamsett[78,ag], K. G. Tan[87], J. Tanaka[156], R. Tanaka[116], S. Tanaka[132], S. Tanaka[65], A. J. Tanasijczuk[143], K. Tani[66], N. Tannoury[84], S. Tapprogge[82], S. Tarem[153], F. Tarrade[29], G. F. Tartarelli[90a], P. Tas[128], M. Tasevsky[126], T. Tashiro[67], E. Tassi[37a,37b], A. Tavares Delgado[125a,125b], Y. Tayalati[136d], C. Taylor[77], F. E. Taylor[93], G. N. Taylor[87], W. Taylor[160b], F. A. Teischinger[30], M. Teixeira Dias Castanheira[75], P. Teixeira-Dias[76], K. K. Temming[48], H. Ten Kate[30], P. K. Teng[152], S. Terada[65], K. Terashi[156], J. Terron[81], S. Terzo[100], M. Testa[47], R. J. Teuscher[159,i], J. Therhaag[21], T. Theveneaux-Pelzer[34], S. Thoma[48], J. P. Thomas[18], J. Thomas-Wilsker[76], E. N. Thompson[35], P. D. Thompson[18], P. D. Thompson[159], A. S. Thompson[53], L. A. Thomsen[36], E. Thomson[121], M. Thomson[28], W. M. Thong[87], R. P. Thun[88,*], F. Tian[35], M. J. Tibbetts[15], V. O. Tikhomirov[95,ah], Yu. A. Tikhonov[108,r], S. Timoshenko[97], E. Tiouchichine[84], P. Tipton[177], S. Tisserant[84], T. Todorov[5], S. Todorova-Nova[128], B. Toggerson[164], J. Tojo[69], S. Tokár[145a], K. Tokushuku[65], K. Tollefson[89], L. Tomlinson[83], M. Tomoto[102], L. Tompkins[31], K. Toms[104], N. D. Topilin[64], E. Torrence[115], H. Torres[143], E. Torró Pastor[168], J. Toth[84,ac], F. Touchard[84], D. R. Tovey[140], H. L. Tran[116], T. Trefzger[175], L. Tremblet[30], A. Tricoli[30], I. M. Trigger[160a], S. Trincaz-Duvoid[79], M. F. Tripiana[70], N. Triplett[25], W. Trischuk[159], B. Trocmé[55], C. Troncon[90a], M. Trottier-McDonald[143], M. Trovatelli[135a,135b], P. True[89], M. Trzebinski[39], A. Trzupek[39], C. Tsarouchas[30], J.C-L. Tseng[119], P. V. Tsiareshka[91], D. Tsionou[137], G. Tsipolitis[10], N. Tsirintanis[9], S. Tsiskaridze[12], V. Tsiskaridze[48], E. G. Tskhadadze[51a], I. I. Tsukerman[96], V. Tsulaia[15], S. Tsuno[65], D. Tsybychev[149], A. Tua[140], A. Tudorache[26a], V. Tudorache[26a], A. N. Tuna[121], S. A. Tupputi[20a,20b], S. Turchikhin[98,af], D. Turecek[127], I. Turk Cakir[4d], R. Turra[90a,90b], P. M. Tuts[35], A. Tykhonov[74], M. Tylmad[147a,147b], M. Tyndel[130], K. Uchida[21], I. Ueda[156], R. Ueno[29], M. Ughetto[84], M. Ugland[14], M. Uhlenbrock[21], F. Ukegawa[161], G. Unal[30], A. Undrus[25], G. Unel[164], F. C. Ungaro[48], Y. Unno[65], D. Urbaniec[35], P. Urquijo[21], G. Usai[8], A. Usanova[61], L. Vacavant[84], V. Vacek[127], B. Vachon[86], N. Valencic[106], S. Valentinetti[20a,20b], A. Valero[168], L. Valery[34], S. Valkar[128], E. Valladolid Gallego[168], S. Vallecorsa[49], J. A. Valls Ferrer[168], P. C. Van Der Deijl[106], R. van der Geer[106], H. van der Graaf[106], R. Van Der Leeuw[106], D. van der Ster[30], N. van Eldik[30], P. van Gemmeren[6], J. Van Nieuwkoop[143], I. van Vulpen[106], M. C. van Woerden[30], M. Vanadia[133a,133b], W. Vandelli[30], A. Vaniachine[6], P. Vankov[42], F. Vannucci[79], G. Vardanyan[178], R. Vari[133a], E. W. Varnes[7], T. Varol[85], D. Varouchas[79], A. Vartapetian[8], K. E. Varvell[151], F. Vazeille[34], T. Vazquez Schroeder[54], J. Veatch[7], F. Veloso[125a,125c], S. Veneziano[133a], A. Ventura[72a,72b], D. Ventura[85], M. Venturi[48], N. Venturi[159], A. Venturini[23], V. Vercesi[120a], M. Verducci[139], W. Verkerke[106], J. C. Vermeulen[106], A. Vest[44], M. C. Vetterli[143,d], O. Viazlo[80], I. Vichou[166], T. Vickey[146c,ai], O. E. Vickey Boeriu[146c], G. H. A. Viehhauser[119], S. Viel[169], R. Vigne[30], M. Villa[20a,20b], M. Villaplana Perez[168], E. Vilucchi[47], M. G. Vincter[29], V. B. Vinogradov[64], J. Virzi[15], O. Vitells[173], I. Vivarelli[150], F. Vives Vaque[3], S. Vlachos[10], D. Vladoiu[99], M. Vlasak[127], A. Vogel[21], P. Vokac[127], G. Volpi[123a,123b], M. Volpi[87], H. von der Schmitt[100], H. von Radziewski[48], E. von Toerne[21], V. Vorobel[128], M. Vos[168], R. Voss[30], J. H. Vossebeld[73], N. Vranjes[137], M. Vranjes Milosavljevic[106], V. Vrba[126], M. Vreeswijk[106], T. Vu Anh[48], R. Vuillermet[30], I. Vukotic[31], Z. Vykydal[127], P. Wagner[21], W. Wagner[176], S. Wahrmund[44], J. Wakabayashi[102], J. Walder[71], R. Walker[99], W. Walkowiak[142], R. Wall[177], P. Waller[73], B. Walsh[177], C. Wang[152,aj], C. Wang[45], F. Wang[174], H. Wang[15], H. Wang[40], J. Wang[42], J. Wang[33a], K. Wang[86], R. Wang[104], S. M. Wang[152], T. Wang[21], X. Wang[177], A. Warburton[86], C. P. Ward[28], D. R. Wardrope[77], M. Warsinsky[48], A. Washbrook[46], C. Wasicki[42], I. Watanabe[66], P. M. Watkins[18], A. T. Watson[18], I. J. Watson[151], M. F. Watson[18], G. Watts[139], S. Watts[83], B. M. Waugh[77], S. Webb[83], M. S. Weber[17], S. W. Weber[175], J. S. Webster[31], A. R. Weidberg[119], P. Weigell[100], B. Weinert[60], J. Weingarten[54], C. Weiser[48], H. Weits[106], P. S. Wells[30], T. Wenaus[25], D. Wendland[16], Z. Weng[152,u], T. Wengler[30], S. Wenig[30], N. Wermes[21], M. Werner[48], P. Werner[30], M. Wessels[58a], J. Wetter[162], K. Whalen[29], A. White[8], M. J. White[1], R. White[32b],

S. White[123a,123b], D. Whiteson[164], D. Wicke[176], F. J. Wickens[130], W. Wiedenmann[174], M. Wielers[130], P. Wienemann[21], C. Wiglesworth[36], L. A. M. Wiik-Fuchs[21], P. A. Wijeratne[77], A. Wildauer[100], M. A. Wildt[42,ak], H. G. Wilkens[30], J. Z. Will[99], H. H. Williams[121], S. Williams[28], C. Willis[89], S. Willocq[85], A. Wilson[88], J. A. Wilson[18], I. Wingerter-Seez[5], S. Winkelmann[48], F. Winklmeier[115], M. Wittgen[144], T. Wittig[43], J. Wittkowski[99], S. J. Wollstadt[82], M. W. Wolter[39], H. Wolters[125a,125c], B. K. Wosiek[39], J. Wotschack[30], M. J. Woudstra[83], K. W. Wozniak[39], M. Wright[53], S. L. Wu[174], X. Wu[49], Y. Wu[88], E. Wulf[35], T. R. Wyatt[83], B. M. Wynne[46], S. Xella[36], M. Xiao[137], D. Xu[33a], L. Xu[33b,al], B. Yabsley[151], S. Yacoob[146b,am], M. Yamada[65], H. Yamaguchi[156], Y. Yamaguchi[156], A. Yamamoto[65], K. Yamamoto[63], S. Yamamoto[156], T. Yamamura[156], T. Yamanaka[156], K. Yamauchi[102], Y. Yamazaki[66], Z. Yan[22], H. Yang[33e], H. Yang[174], U. K. Yang[83], Y. Yang[110], S. Yanush[92], L. Yao[33a], W-M. Yao[15], Y. Yasu[65], E. Yatsenko[42], K. H. Yau Wong[21], J. Ye[40], S. Ye[25], A. L. Yen[57], E. Yildirim[42], M. Yilmaz[4b], R. Yoosoofmiya[124], K. Yorita[172], R. Yoshida[6], K. Yoshihara[156], C. Young[144], C. J. S. Young[30], S. Youssef[22], D. R. Yu[15], J. Yu[8], J. M. Yu[88], J. Yu[113], L. Yuan[66], A. Yurkewicz[107], B. Zabinski[39], R. Zaidan[62], A. M. Zaitsev[129,z], A. Zaman[149], S. Zambito[23], L. Zanello[133a,133b], D. Zanzi[100], A. Zaytsev[25], C. Zeitnitz[176], M. Zeman[127], A. Zemla[38a], K. Zengel[23], O. Zenin[129], T. Ženiš[145a], D. Zerwas[116], G. Zevi della Porta[57], D. Zhang[88], F. Zhang[174], H. Zhang[89], J. Zhang[6], L. Zhang[152], X. Zhang[33d], Z. Zhang[116], Z. Zhao[33b], A. Zhemchugov[64], J. Zhong[119], B. Zhou[88], L. Zhou[35], N. Zhou[164], C. G. Zhu[33d], H. Zhu[33a], J. Zhu[88], Y. Zhu[33b], X. Zhuang[33a], A. Zibell[99], D. Zieminska[60], N. I. Zimine[64], C. Zimmermann[82], R. Zimmermann[21], S. Zimmermann[21], S. Zimmermann[48], Z. Zinonos[54], M. Ziolkowski[142], R. Zitoun[5], G. Zobernig[174], A. Zoccoli[20a,20b], M. zur Nedden[16], G. Zurzolo[103a,103b], V. Zutshi[107], L. Zwalinski[30]

[1] Department of Physics, University of Adelaide, Adelaide, Australia
[2] Physics Department, SUNY Albany, Albany, NY, USA
[3] Department of Physics, University of Alberta, Edmonton, AB, Canada
[4] (a) Department of Physics, Ankara University, Ankara, Turkey; (b) Department of Physics, Gazi University, Ankara, Turkey; (c) Division of Physics, TOBB University of Economics and Technology, Ankara, Turkey; (d) Turkish Atomic Energy Authority, Ankara, Turkey
[5] LAPP, CNRS/IN2P3 and Université de Savoie, Annecy-le-Vieux, France
[6] High Energy Physics Division, Argonne National Laboratory, Argonne, IL, USA
[7] Department of Physics, University of Arizona, Tucson, AZ, USA
[8] Department of Physics, The University of Texas at Arlington, Arlington, TX, USA
[9] Physics Department, University of Athens, Athens, Greece
[10] Physics Department, National Technical University of Athens, Zografou, Athens, Greece
[11] Institute of Physics, Azerbaijan Academy of Sciences, Baku, Azerbaijan
[12] Institut de Física d'Altes Energies and Departament de Física de la Universitat Autònoma de Barcelona, Barcelona, Spain
[13] (a) Institute of Physics, University of Belgrade, Belgrade, Serbia; (b) Vinca Institute of Nuclear Sciences, University of Belgrade, Belgrade, Serbia
[14] Department for Physics and Technology, University of Bergen, Bergen, Norway
[15] Physics Division, Lawrence Berkeley National Laboratory and University of California, Berkeley, CA, USA
[16] Department of Physics, Humboldt University, Berlin, Germany
[17] Albert Einstein Center for Fundamental Physics and Laboratory for High Energy Physics, University of Bern, Bern, Switzerland
[18] School of Physics and Astronomy, University of Birmingham, Birmingham, UK
[19] (a) Department of Physics, Bogazici University, Istanbul, Turkey; (b) Department of Physics, Dogus University, Istanbul, Turkey; (c) Department of Physics Engineering, Gaziantep University, Gaziantep, Turkey
[20] (a) INFN Sezione di Bologna, Bologna, Italy; (b) Dipartimento di Fisica e Astronomia, Università di Bologna, Bologna, Italy
[21] Physikalisches Institut, University of Bonn, Bonn, Germany
[22] Department of Physics, Boston University, Boston, MA, USA
[23] Department of Physics, Brandeis University, Waltham, MA, USA
[24] (a) Universidade Federal do Rio De Janeiro COPPE/EE/IF, Rio de Janeiro, Brazil; (b) Federal University of Juiz de Fora (UFJF), Juiz de Fora, Brazil; (c) Federal University of Sao Joao del Rei (UFSJ), Sao Joao del Rei, Brazil; (d) Instituto de Fisica, Universidade de Sao Paulo, São Paulo, Brazil
[25] Physics Department, Brookhaven National Laboratory, Upton, NY, USA

[26] [(a)] National Institute of Physics and Nuclear Engineering, Bucharest, Romania; [(b)] Physics Department, National Institute for Research and Development of Isotopic and Molecular Technologies, Cluj Napoca, Romania; [(c)] University Politehnica Bucharest, Bucharest, Romania; [(d)] West University in Timisoara, Timisoara, Romania
[27] Departamento de Física, Universidad de Buenos Aires, Buenos Aires, Argentina
[28] Cavendish Laboratory, University of Cambridge, Cambridge, UK
[29] Department of Physics, Carleton University, Ottawa, ON, Canada
[30] CERN, Geneva, Switzerland
[31] Enrico Fermi Institute, University of Chicago, Chicago, IL, USA
[32] [(a)] Departamento de Física, Pontificia Universidad Católica de Chile, Santiago, Chile; [(b)] Departamento de Física, Universidad Técnica Federico Santa María, Valparaiso, Chile
[33] [(a)] Institute of High Energy Physics, Chinese Academy of Sciences, Beijing, China; [(b)] Department of Modern Physics, University of Science and Technology of China, Hefei, Anhui, China; [(c)] Department of Physics, Nanjing University, Nanjing, Jiangsu, China; [(d)] School of Physics, Shandong University, Jinan, Shandong, China; [(e)] Physics Department, Shanghai Jiao Tong University, Shanghai, China
[34] Laboratoire de Physique Corpusculaire, Clermont Université and Université Blaise Pascal and CNRS/IN2P3, Clermont-Ferrand, France
[35] Nevis Laboratory, Columbia University, Irvington, NY, USA
[36] Niels Bohr Institute, University of Copenhagen, Copenhagen, Denmark
[37] [(a)] INFN Gruppo Collegato di Cosenza, Laboratori Nazionali di Frascati, Frascati, Italy; [(b)] Dipartimento di Fisica, Università della Calabria, Rende, Italy
[38] [(a)] Faculty of Physics and Applied Computer Science, AGH University of Science and Technology, Kraków, Poland; [(b)] Marian Smoluchowski Institute of Physics, Jagiellonian University, Kraków, Poland
[39] The Henryk Niewodniczanski Institute of Nuclear Physics, Polish Academy of Sciences, Kraków, Poland
[40] Physics Department, Southern Methodist University, Dallas, TX, USA
[41] Physics Department, University of Texas at Dallas, Richardson, TX, USA
[42] DESY, Hamburg and Zeuthen, Germany
[43] Institut für Experimentelle Physik IV, Technische Universität Dortmund, Dortmund, Germany
[44] Institut für Kern- und Teilchenphysik, Technische Universität Dresden, Dresden, Germany
[45] Department of Physics, Duke University, Durham, NC, USA
[46] SUPA-School of Physics and Astronomy, University of Edinburgh, Edinburgh, UK
[47] INFN Laboratori Nazionali di Frascati, Frascati, Italy
[48] Fakultät für Mathematik und Physik, Albert-Ludwigs-Universität, Freiburg, Germany
[49] Section de Physique, Université de Genève, Geneva, Switzerland
[50] [(a)] INFN Sezione di Genova, Genoa, Italy; [(b)] Dipartimento di Fisica, Università di Genova, Genoa, Italy
[51] [(a)] E. Andronikashvili Institute of Physics, Iv. Javakhishvili Tbilisi State University, Tbilisi, Georgia; [(b)] High Energy Physics Institute, Tbilisi State University, Tbilisi, Georgia
[52] II Physikalisches Institut, Justus-Liebig-Universität Giessen, Giessen, Germany
[53] SUPA-School of Physics and Astronomy, University of Glasgow, Glasgow, UK
[54] II Physikalisches Institut, Georg-August-Universität, Göttingen, Germany
[55] Laboratoire de Physique Subatomique et de Cosmologie, Université Grenoble-Alpes, CNRS/IN2P3, Grenoble, France
[56] Department of Physics, Hampton University, Hampton, VA, USA
[57] Laboratory for Particle Physics and Cosmology, Harvard University, Cambridge, MA, USA
[58] [(a)] Kirchhoff-Institut für Physik, Ruprecht-Karls-Universität Heidelberg, Heidelberg, Germany; [(b)] Physikalisches Institut, Ruprecht-Karls-Universität Heidelberg, Heidelberg, Germany; [(c)] ZITI Institut für technische Informatik, Ruprecht-Karls-Universität Heidelberg, Mannheim, Germany
[59] Faculty of Applied Information Science, Hiroshima Institute of Technology, Hiroshima, Japan
[60] Department of Physics, Indiana University, Bloomington, IN, USA
[61] Institut für Astro- und Teilchenphysik, Leopold-Franzens-Universität, Innsbruck, Austria
[62] University of Iowa, Iowa City, IA, USA
[63] Department of Physics and Astronomy, Iowa State University, Ames, IA, USA
[64] Joint Institute for Nuclear Research, JINR Dubna, Dubna, Russia
[65] KEK, High Energy Accelerator Research Organization, Tsukuba, Japan
[66] Graduate School of Science, Kobe University, Kobe, Japan

[67] Faculty of Science, Kyoto University, Kyoto, Japan
[68] Kyoto University of Education, Kyoto, Japan
[69] Department of Physics, Kyushu University, Fukuoka, Japan
[70] Instituto de Física La Plata, Universidad Nacional de La Plata and CONICET, La Plata, Argentina
[71] Physics Department, Lancaster University, Lancaster, UK
[72] [(a)] INFN Sezione di Lecce, Lecce, Italy; [(b)] Dipartimento di Matematica e Fisica, Università del Salento, Lecce, Italy
[73] Oliver Lodge Laboratory, University of Liverpool, Liverpool, UK
[74] Department of Physics, Jožef Stefan Institute and University of Ljubljana, Ljubljana, Slovenia
[75] School of Physics and Astronomy, Queen Mary University of London, London, UK
[76] Department of Physics, Royal Holloway University of London, Surrey, UK
[77] Department of Physics and Astronomy, University College London, London, UK
[78] Louisiana Tech University, Ruston, LA, USA
[79] Laboratoire de Physique Nucléaire et de Hautes Energies, UPMC and Université Paris-Diderot and CNRS/IN2P3, Paris, France
[80] Fysiska institutionen, Lunds universitet, Lund, Sweden
[81] Departamento de Fisica Teorica C-15, Universidad Autonoma de Madrid, Madrid, Spain
[82] Institut für Physik, Universität Mainz, Mainz, Germany
[83] School of Physics and Astronomy, University of Manchester, Manchester, UK
[84] CPPM, Aix-Marseille Université and CNRS/IN2P3, Marseille, France
[85] Department of Physics, University of Massachusetts, Amherst, MA, USA
[86] Department of Physics, McGill University, Montreal, QC, Canada
[87] School of Physics, University of Melbourne, Parkville, VIC, Australia
[88] Department of Physics, The University of Michigan, Ann Arbor, MI, USA
[89] Department of Physics and Astronomy, Michigan State University, East Lansing, MI, USA
[90] [(a)] INFN Sezione di Milano, Milan, Italy; [(b)] Dipartimento di Fisica, Università di Milano, Milan, Italy
[91] B.I. Stepanov Institute of Physics, National Academy of Sciences of Belarus, Minsk, Republic of Belarus
[92] National Scientific and Educational Centre for Particle and High Energy Physics, Minsk, Republic of Belarus
[93] Department of Physics, Massachusetts Institute of Technology, Cambridge, MA, USA
[94] Group of Particle Physics, University of Montreal, Montreal, QC, Canada
[95] P.N. Lebedev Institute of Physics, Academy of Sciences, Moscow, Russia
[96] Institute for Theoretical and Experimental Physics (ITEP), Moscow, Russia
[97] Moscow Engineering and Physics Institute (MEPhI), Moscow, Russia
[98] D.V.Skobeltsyn Institute of Nuclear Physics, M.V.Lomonosov Moscow State University, Moscow, Russia
[99] Fakultät für Physik, Ludwig-Maximilians-Universität München, Munich, Germany
[100] Max-Planck-Institut für Physik (Werner-Heisenberg-Institut), Munich, Germany
[101] Nagasaki Institute of Applied Science, Nagasaki, Japan
[102] Graduate School of Science and Kobayashi-Maskawa Institute, Nagoya University, Nagoya, Japan
[103] [(a)] INFN Sezione di Napoli, Naples, Italy; [(b)] Dipartimento di Fisica, Università di Napoli, Naples, Italy
[104] Department of Physics and Astronomy, University of New Mexico, Albuquerque, NM, USA
[105] Institute for Mathematics, Astrophysics and Particle Physics, Radboud University Nijmegen/Nikhef, Nijmegen, The Netherlands
[106] Nikhef National Institute for Subatomic Physics and University of Amsterdam, Amsterdam, The Netherlands
[107] Department of Physics, Northern Illinois University, DeKalb, IL, USA
[108] Budker Institute of Nuclear Physics, SB RAS, Novosibirsk, Russia
[109] Department of Physics, New York University, New York, NY, USA
[110] Ohio State University, Columbus, OH, USA
[111] Faculty of Science, Okayama University, Okayama, Japan
[112] Homer L. Dodge Department of Physics and Astronomy, University of Oklahoma, Norman, OK, USA
[113] Department of Physics, Oklahoma State University, Stillwater, OK, USA
[114] Palacký University, RCPTM, Olomouc, Czech Republic
[115] Center for High Energy Physics, University of Oregon, Eugene, OR, USA
[116] LAL, Université Paris-Sud and CNRS/IN2P3, Orsay, France
[117] Graduate School of Science, Osaka University, Osaka, Japan

[118] Department of Physics, University of Oslo, Oslo, Norway
[119] Department of Physics, Oxford University, Oxford, UK
[120] [(a)] INFN Sezione di Pavia, Pavia, Italy; [(b)] Dipartimento di Fisica, Università di Pavia, Pavia, Italy
[121] Department of Physics, University of Pennsylvania, Philadelphia, PA, USA
[122] Petersburg Nuclear Physics Institute, Gatchina, Russia
[123] [(a)] INFN Sezione di Pisa, Pisa, Italy; [(b)] Dipartimento di Fisica E. Fermi, Università di Pisa, Pisa, Italy
[124] Department of Physics and Astronomy, University of Pittsburgh, Pittsburgh, PA, USA
[125] [(a)] Laboratorio de Instrumentacao e Fisica Experimental de Particulas-LIP, Lisbon, Portugal; [(b)] Faculdade de Ciências, Universidade de Lisboa, Lisbon, Portugal; [(c)] Department of Physics, University of Coimbra, Coimbra, Portugal; [(d)] Centro de Física Nuclear da Universidade de Lisboa, Lisbon, Portugal; [(e)] Departamento de Fisica, Universidade do Minho, Braga, Portugal; [(f)] Departamento de Fisica Teorica y del Cosmos and CAFPE, Universidad de Granada, Granada, Spain; [(g)] Dep Fisica and CEFITEC of Faculdade de Ciencias e Tecnologia, Universidade Nova de Lisboa, Caparica, Portugal
[126] Institute of Physics, Academy of Sciences of the Czech Republic, Prague, Czech Republic
[127] Czech Technical University in Prague, Prague, Czech Republic
[128] Faculty of Mathematics and Physics, Charles University in Prague, Prague, Czech Republic
[129] State Research Center Institute for High Energy Physics, Protvino, Russia
[130] Particle Physics Department, Rutherford Appleton Laboratory, Didcot, UK
[131] Physics Department, University of Regina, Regina, SK, Canada
[132] Ritsumeikan University, Kusatsu, Shiga, Japan
[133] [(a)] INFN Sezione di Roma, Rome, Italy; [(b)] Dipartimento di Fisica, Sapienza Università di Roma, Rome, Italy
[134] [(a)] INFN Sezione di Roma Tor Vergata, Rome, Italy; [(b)] Dipartimento di Fisica, Università di Roma Tor Vergata, Rome, Italy
[135] [(a)] INFN Sezione di Roma Tre, Rome, Italy; [(b)] Dipartimento di Matematica e Fisica, Università Roma Tre, Rome, Italy
[136] [(a)] Faculté des Sciences Ain Chock, Réseau Universitaire de Physique des Hautes Energies-Université Hassan II, Casablanca, Morocco; [(b)] Centre National de l'Energie des Sciences Techniques Nucleaires, Rabat, Morocco; [(c)] Faculté des Sciences Semlalia, Université Cadi Ayyad, LPHEA-Marrakech, Marrakech, Morocco; [(d)] Faculté des Sciences, Université Mohamed Premier and LPTPM, Oujda, Morocco; [(e)] Faculté des Sciences, Université Mohammed V-Agdal, Rabat, Morocco
[137] DSM/IRFU (Institut de Recherches sur les Lois Fondamentales de l'Univers), CEA Saclay (Commissariat à l'Energie Atomique et aux Energies Alternatives), Gif-sur-Yvette, France
[138] Santa Cruz Institute for Particle Physics, University of California Santa Cruz, Santa Cruz, CA, USA
[139] Department of Physics, University of Washington, Seattle, WA, USA
[140] Department of Physics and Astronomy, University of Sheffield, Sheffield, UK
[141] Department of Physics, Shinshu University, Nagano, Japan
[142] Fachbereich Physik, Universität Siegen, Siegen, Germany
[143] Department of Physics, Simon Fraser University, Burnaby, BC, Canada
[144] SLAC National Accelerator Laboratory, Stanford, CA, USA
[145] [(a)] Faculty of Mathematics, Physics and Informatics, Comenius University, Bratislava, Slovak Republic; [(b)] Department of Subnuclear Physics, Institute of Experimental Physics of the Slovak Academy of Sciences, Kosice, Slovak Republic
[146] [(a)] Department of Physics, University of Cape Town, Cape Town, South Africa; [(b)] Department of Physics, University of Johannesburg, Johannesburg, South Africa; [(c)] School of Physics, University of the Witwatersrand, Johannesburg, South Africa
[147] [(a)] Department of Physics, Stockholm University, Stockholm, Sweden; [(b)] The Oskar Klein Centre, Stockholm, Sweden
[148] Physics Department, Royal Institute of Technology, Stockholm, Sweden
[149] Departments of Physics and Astronomy and Chemistry, Stony Brook University, Stony Brook, NY, USA
[150] Department of Physics and Astronomy, University of Sussex, Brighton, UK
[151] School of Physics, University of Sydney, Sydney, Australia
[152] Institute of Physics, Academia Sinica, Taipei, Taiwan
[153] Department of Physics, Technion: Israel Institute of Technology, Haifa, Israel
[154] Raymond and Beverly Sackler School of Physics and Astronomy, Tel Aviv University, Tel Aviv, Israel
[155] Department of Physics, Aristotle University of Thessaloniki, Thessaloniki, Greece
[156] International Center for Elementary Particle Physics and Department of Physics, The University of Tokyo, Tokyo, Japan

[157] Graduate School of Science and Technology, Tokyo Metropolitan University, Tokyo, Japan
[158] Department of Physics, Tokyo Institute of Technology, Tokyo, Japan
[159] Department of Physics, University of Toronto, Toronto, ON, Canada
[160] [(a)] TRIUMF, Vancouver, BC, Canada; [(b)] Department of Physics and Astronomy, York University, Toronto, ON, Canada
[161] Faculty of Pure and Applied Sciences, University of Tsukuba, Tsukuba, Japan
[162] Department of Physics and Astronomy, Tufts University, Medford, MA, USA
[163] Centro de Investigaciones, Universidad Antonio Narino, Bogota, Colombia
[164] Department of Physics and Astronomy, University of California Irvine, Irvine, CA, USA
[165] [(a)] INFN Gruppo Collegato di Udine, Sezione di Trieste, Udine, Italy; [(b)] ICTP, Trieste, Italy; [(c)] Dipartimento di Chimica, Fisica e Ambiente, Università di Udine, Udine, Italy
[166] Department of Physics, University of Illinois, Urbana, IL, USA
[167] Department of Physics and Astronomy, University of Uppsala, Uppsala, Sweden
[168] Instituto de Física Corpuscular (IFIC) and Departamento de Física Atómica, Molecular y Nuclear and Departamento de Ingeniería Electrónica and Instituto de Microelectrónica de Barcelona (IMB-CNM), University of Valencia and CSIC, Valencia, Spain
[169] Department of Physics, University of British Columbia, Vancouver, BC, Canada
[170] Department of Physics and Astronomy, University of Victoria, Victoria, BC, Canada
[171] Department of Physics, University of Warwick, Coventry, UK
[172] Waseda University, Tokyo, Japan
[173] Department of Particle Physics, The Weizmann Institute of Science, Rehovot, Israel
[174] Department of Physics, University of Wisconsin, Madison, WI, USA
[175] Fakultät für Physik und Astronomie, Julius-Maximilians-Universität, Würzburg, Germany
[176] Fachbereich C Physik, Bergische Universität Wuppertal, Wuppertal, Germany
[177] Department of Physics, Yale University, New Haven, CT, USA
[178] Yerevan Physics Institute, Yerevan, Armenia
[179] Centre de Calcul de l'Institut National de Physique Nucléaire et de Physique des Particules (IN2P3), Villeurbanne, France

[a] Also at Department of Physics, King's College London, London, UK
[b] Also at Institute of Physics, Azerbaijan Academy of Sciences, Baku, Azerbaijan
[c] Also at Particle Physics Department, Rutherford Appleton Laboratory, Didcot, UK
[d] Also at TRIUMF, Vancouver, BC, Canada
[e] Also at Department of Physics, California State University, Fresno, CA, USA
[f] Also at Tomsk State University, Tomsk, Russia
[g] Also at CPPM, Aix-Marseille Université and CNRS/IN2P3, Marseille, France
[h] Also at Università di Napoli Parthenope, Naples, Italy
[i] Also at Institute of Particle Physics (IPP), Canada
[j] Also at Department of Physics, St. Petersburg State Polytechnical University, St. Petersburg, Russia
[k] Also at Chinese University of Hong Kong, China
[l] Also at Department of Financial and Management Engineering, University of the Aegean, Chios, Greece
[m] Also at Louisiana Tech University, Ruston, LA, USA
[n] Also at Institucio Catalana de Recerca i Estudis Avancats, ICREA, Barcelona, Spain
[o] Also at CERN, Geneva, Switzerland
[p] Also at Ochadai Academic Production, Ochanomizu University, Tokyo, Japan
[q] Also at Manhattan College, New York, NY, USA
[r] Also at Novosibirsk State University, Novosibirsk, Russia
[s] Also at Institute of Physics, Academia Sinica, Taipei, Taiwan
[t] Also at LAL, Université Paris-Sud and CNRS/IN2P3, Orsay, France
[u] Also at School of Physics and Engineering, Sun Yat-sen University, Guangzhou, China
[v] Also at Academia Sinica Grid Computing, Institute of Physics, Academia Sinica, Taipei, Taiwan
[w] Also at Laboratoire de Physique Nucléaire et de Hautes Energies, UPMC and Université Paris-Diderot and CNRS/IN2P3, Paris, France
[x] Also at School of Physical Sciences, National Institute of Science Education and Research, Bhubaneswar, India
[y] Also at Dipartimento di Fisica, Sapienza Università di Roma, Rome, Italy

[z] Also at Moscow Institute of Physics and Technology State University, Dolgoprudny, Russia
[aa] Also at Section de Physique, Université de Genève, Geneva, Switzerland
[ab] Also at Department of Physics, The University of Texas at Austin, Austin, TX, USA
[ac] Also at Institute for Particle and Nuclear Physics, Wigner Research Centre for Physics, Budapest, Hungary
[ad] Also at International School for Advanced Studies (SISSA), Trieste, Italy
[ae] Also at Department of Physics and Astronomy, University of South Carolina, Columbia, SC, USA
[af] Also at Faculty of Physics, M.V.Lomonosov Moscow State University, Moscow, Russia
[ag] Also at Physics Department, Brookhaven National Laboratory, Upton, NY, USA
[ah] Also at Moscow Engineering and Physics Institute (MEPhI), Moscow, Russia
[ai] Also at Department of Physics, Oxford University, Oxford, UK
[aj] Also at Department of Physics, Nanjing University, Jiangsu, China
[ak] Also at Institut für Experimentalphysik, Universität Hamburg, Hamburg, Germany
[al] Also at Department of Physics, The University of Michigan, Ann Arbor, MI, USA
[am] Also at Discipline of Physics, University of KwaZulu-Natal, Durban, South Africa
* Deceased